Urban morphological analysis for wind potential

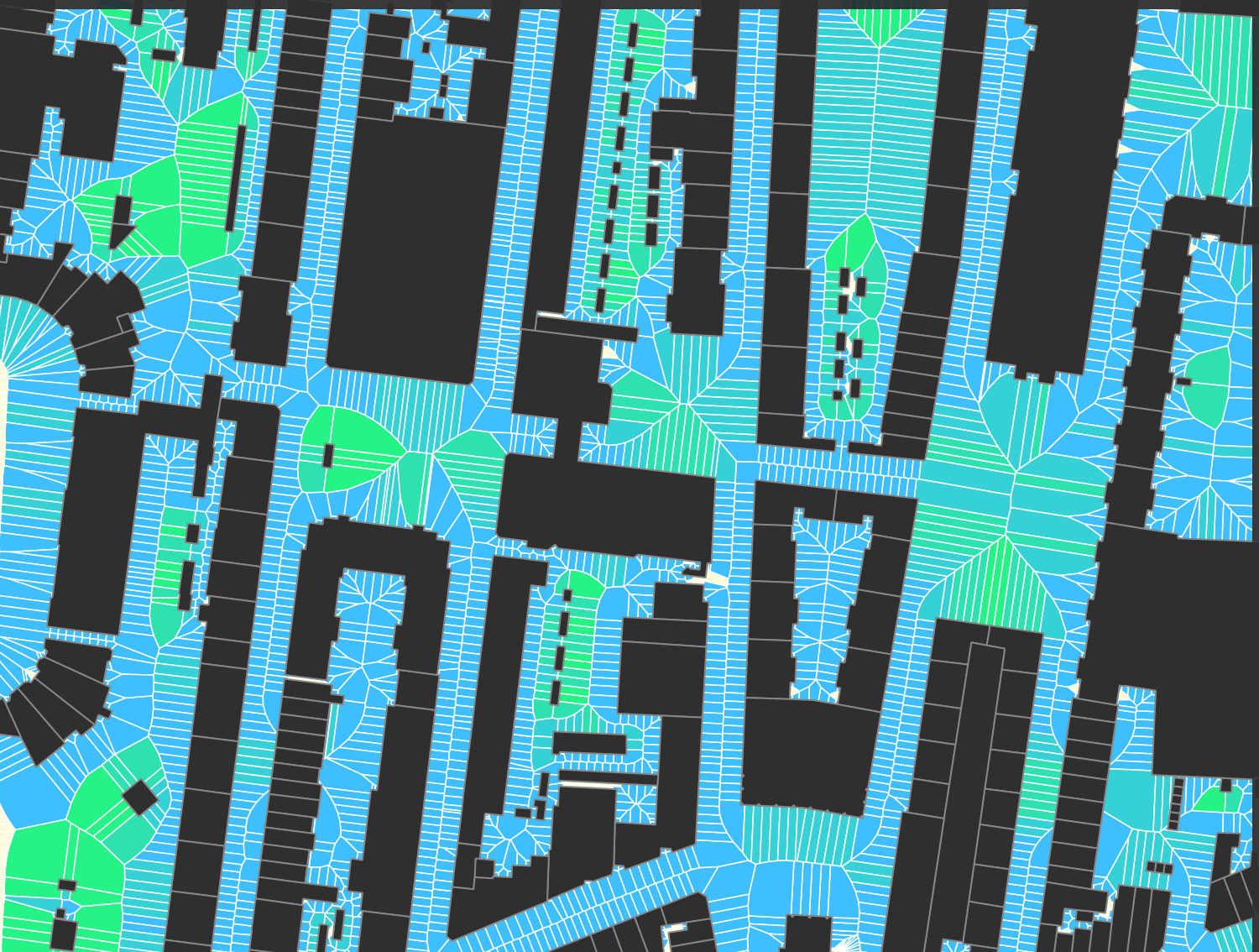

W. (Wessel) T. de Jongh, BSc

MSc Thesis in Geomatics

June 2021

TU Delft

URBAN MORPHOLOGICAL ANALYSIS FOR WIND POTENTIAL

A thesis submitted to the Delft University of Technology in partial fulfillment of the requirements for the degree of

Master of Science in Geomatics for the Built Environment

by

Wessel de Jongh

June 2021

The work in this thesis was carried out in the:

3D geoinformation group
Department of Urbanism
Faculty of the Built Environment & Architecture
Delft University of Technology

Supervisors:	Asst. Prof. Dr. Clara García-Sańchez
	Ir. Balàzs Dukai
Co-reader:	Ir. Daniela Maiullari

ABSTRACT

Wind has a profound impact on the meteorological and environmental conditions in cities. And so, by understanding wind flow behaviour within the urban environment, we can use the increasingly available open data to contribute to the design of healthy cities. This Master's thesis present a methodology to compute urban morphological parameters and its effect on potential wind velocity. The proposed method may serve as an complementary method to Computational Fluid Dynamics (CFD) simulation or scaled wind tunnel tests. The research question in this thesis is: *Can we use urban morphology to automatically calculate potential increase in wind velocity?* To answer this, first an introduction to wind flows in the urban environment is presented. Then, several methodologies are presented to compute the urban morphological parameters, such as the Urban Canyon, wind- or leeward facade, Angle of Attack and terrain roughness length. The method relies on the use of a Voronoi diagram, with cells describing the morphology. After, the urban morphological parameters are related to potential wind velocity through a scoring method. Using two meteorological stations inside the area of interest, the mean wind velocity is compared to the scores. The result show that both stations show a higher mean wind velocity for higher scores. However, more research is necessary to validate this outcome and a recommendation is given to compare the result of this thesis to a CFD simulation.

ACKNOWLEDGEMENTS

First, I would like to show my appreciation by thanking Clara García-Sańchez, my main supervisor, for her indispensable knowledge and help but also for keeping me motivated by putting (a healthy amount of) pressure on me throughout this Masters' thesis. Second, my second-supervisor Balàzs Dukai for his continuous support, insights and conversations about handling big projects, especially in tough times (CoViD-19). Most of all, I would like to thank them for an incredible collaboration, which has left quite the impression on me. Weekly progression meetings is not something that is usually done, but it helped me push and bring my work to a higher level.

Then, Daniela Maiullari for her enthusiasm about my topic and for providing feedback as my co-reader. I would also like to acknowledge Ype Cuperus, for organising the presentation meetings.

I would like to thank fellow student Bob Spitz, who has helped me make sense of it all and for keeping me sane the past couple of years.

Last, a big thank you to my parents, Marlies Wessels and Chris de Jongh, for backing me up with wise counsel and encouragement whenever I needed.

CONTENTS

LIST OF FIGURES

LIST OF TABLES

List of Algorithms

ACRONYMS

1 INTRODUCTION

Wind flows in the urban environment have been researched extensively over the last few decades. Some of the reasons for the researchers interest in wind flows resides in their influence on Urban Heat Island (UHI), energy consumption, pedestrian wind comfort and air quality, just to name a few. These studies show the importance of understanding the wind flow behaviour within our cities, so that engineers, architects and city planners can design healthy cities.

Thus far, most of the studies have relied on Computational Fluid Dynamics (CFD) simulations, either idealized or based on real situations [Carpentieri and Robins, 2015; Chen et al., 2017; Janssen et al., 2013; Razak et al., 2013], scaled wind tunnel experiments [Tsang et al., 2012; Kubota et al., 2008; Carpentieri and Robins, 2015; Chen et al., 2017] and sometimes street measurements [Oke, 1988; Soulhac et al., 2009; Arnold et al., 2004]. Although these experiments provide an accurate understanding of certain situations, they are more complex and (time-) expensive to perform at a city scale. Therefore, an interesting approach easy to apply during the first stages of design would be to try to induce the flow behaviour from a parametric perspective. A methodology where the key morphological parameters help us to derive the most probably urban wind condition.

Many researchers, like Oke [1988] and others, describe in their articles the influence of urban morphology on wind flows, such as building aspect ratio, presence of tall buildings or floor area density. The research of Jiang et al. [2008] also suggests that wind structure and turbulence profiles can be assessed using morphological parameters. And thanks to access to open data made available by the Dutch governmental agencies and municipalities, computing these parameters is possible. Within this research I investigate how to link urban morphological parameters to the potential increase of wind flows at the city scale.

1.1 OBJECTIVES & RESEARCH QUESTIONS

This thesis aims to explore the methodologies behind computing morphological parameters used in wind flow analysis. By combining these parameters, we can gain new insights as to what combination of parameters may lead to a potential for increased wind velocity in the urban environment. For the purpose of this thesis, the algorithms are only tested in a certain area of interest, but they are applicable to all mayor cities (in the Netherlands). For other countries, a dataset of building footprint enriched with building height information and a map describing open space typology or materials is needed. For a larger area, defined neighborhood zones can be used to speed up computation time for certain algorithms.

The study builds upon previous work by Ceccarelli et al. [2019], where a methodology was proposed to automatically calculate the height and width of urban canyons.

The main research question within this Master thesis is:

- Can we use urban morphology to automatically calculate potential increase in wind velocity?

Additionally, the following sub-questions are defined in order to answer the main question:

1. How do different morphological parameters relate to wind velocity?
2. Is it possible to develop methodologies to automatically calculate multiple morphological parameters?
3. Is this method suitable for identifying potentially increased wind velocity situations?
4. Can we use meteorological measurement stations to validate the methodology?

1.2 FRAME OF RESEARCH

The relevance of this thesis is to create a simplified method in order to quickly assess certain combination of morphological parameters that may cause increase in wind velocity in the urban environment. Current methods do so by means of CFD or down-scaled wind tunnel tests. In both methods, the buildings and environment are used as an input. In CFD, the environment is 3D modelled into a mesh of certain density, whose size is limited by the complexity and the computational power.

The method proposed in this thesis aims to understand wind flows in the urban environment from a morphological point of view. By using algorithms to compute certain geometric properties of the city that have shown to impact wind flows in literature, the urban environment is mapped.

The morphological parameters are then used as indicators for potential increase in wind velocity. As the relationship between the parameters and wind velocity is not clearly defined, I propose a simple approach of scoring the parameters to synthesise potential increase in wind velocity. Then using meteorological data from two stations inside the area of interest, an attempt to validate the scoring approach is done.

1.3 THESIS OUTLINE

The following chapters of this thesis are structured as follows:

In Chapter 2, I discuss the related literature, relevant to this thesis. Here, I aim to introduce the reader to the current (or lack thereof) methodologies of urban wind analysis using geographical informational systems and computational tools. I also dive into the characteristics of the built environment that influence wind flows at pedestrian level.

In Chapter 3, I describe the framework for computing the different parameters relevant to this thesis. As well as explaining the computational approach and methods needed for the calculation of the morphological parameters.

Then in Chapter 4 I explain the different implementations of the computational approach to calculating various morphological parameters.

Followed by Chapter 5, where I present the results from my implementations along with the translation of parameters to wind potential and the validation through the meteorological data comparison.

Finally, in Chapter 6 I will draw the conclusion of this thesis and provide a discussion and limitations section along with a future research recommendation.

2 RELATED WORK AND THEORY

In this chapter, I provide the related work and theory that is relevant to this thesis. First, §2.1 is where I explain different simplified wind flows caused by buildings in the urban environment. In §2.2, I discuss previous studies related to morphological analysis. After, I briefly discuss other related parameters out-of-scope for this thesis. And finally, §2.4 is about the key algorithm that I will be using in the following chapters.

2.1 URBAN WIND FLOWS

I will break down how wind flows are effected by the built environment in four categories, for the purpose of this thesis. The wind flows presented in the following subsections are assumptions and oversimplifications of complex 3-dimensional problems. The simplification is necessary for two reasons: first, because it is relevant from a morphology point of view and second, so that they are understandable and, more importantly, quantifiable.

2.1.1 Tall Buildings

Blocken and Carmeliet [2004] presented a schematic understanding of the different wind flows happening around a single, tall building from Beranek and Koten [1979]. Noticeable in figure 2.1 are 3 important aspects of wind around the building. 1) A high pressure zone and wind flow down the windward face of the building (5), creating a vortex at the foot of the building (6); 2) the vortex joining the main stream (9) at the corner where the difference in pressure causes high wind speeds (8); 3) and lastly, the backwash vortex (13) and low pressure zone at the leeward side of the building.

Tsang et al. [2012] investigated the influence of tall buildings in a parametric wind tunnel study and identified a lateral high wind speed zone at pedestrian level, at the side of the building (fig. 2.2). This is caused by the downwash from the windward facade of the building. The same research also investigated the influence of building height on the pedestrian level wind. Although not explicitly mentioned, the plots

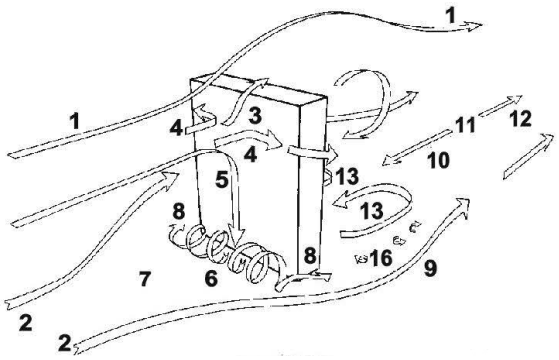

Figure 2.1: A schematic representation of flows encountering a tall rectangular building. Source: [Beranek and Koten, 1979]

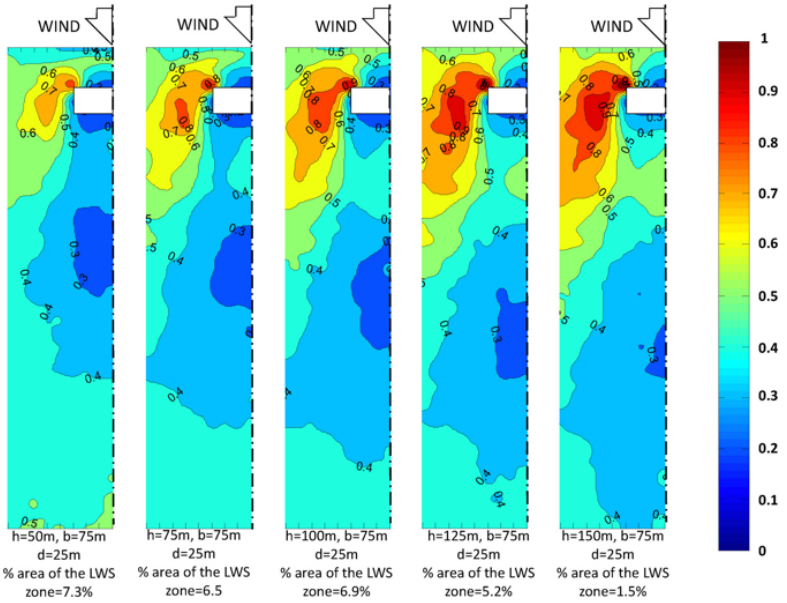

Figure 2.2: Lateral high wind speed zones when encountering a tall building, colors indicate pressure zones, with red color representing high pressure. Source: [Tsang et al., 2012]

of variable building height showed a correlation between the height of the building and the area and intensity of the lateral high wind speed zone. This makes sense, as the wind velocity increases with height logarithmically in a neutral atmospheric boundary layer [Blocken and Carmeliet, 2004].

2.1.2 Urban Canyon

The Urban Canyon (UC) is a parameter that is characterised by the ratio between the height of the buildings (H) and the length (L) and width (W) of the street (fig. 2.3). The ratio between parameters describes the shape of the canyon, where H/W describes the shape of the cross-section of the street, L/W the shape of the floor area of the canyon and L/H the shape of the facade attached to the canyon.

Carpentieri and Robins [2015] have studied the importance and effect of different Aspect Ratio (AR) (also known as H/W), building height variation in combination with wind direction. Oke [1988] describes three different type of flows as a result of the AR: skimming flow, isolated roughness flow and wake interference flow shown in figure 2.4. These types of flow describe how the wind above the canyon interacts with the flow inside the canyon. For very low H/W ratio (<0,05), the wake of the flow over the building more or less stabilizes before the flow interacts with the next building. This, Oke [1988] calls the isolated roughness flow (2.4a). For smaller widths or higher H/W ratio, the turbulence of the upwind building interferes with the windward side of the next building causing a wake interference flow (2.4b).

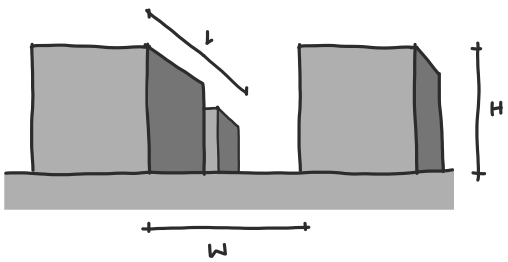

Figure 2.3: Simplification of Urban Canyon

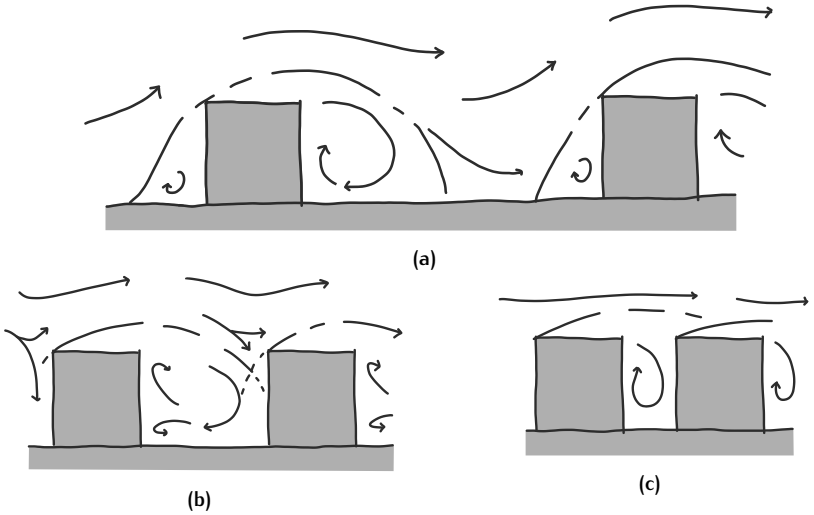

Figure 2.4: Simplification of isolated roughness flow (a), wake interference flow (b) and isolated skimming flow (c). Reproduced from Oke [1988].

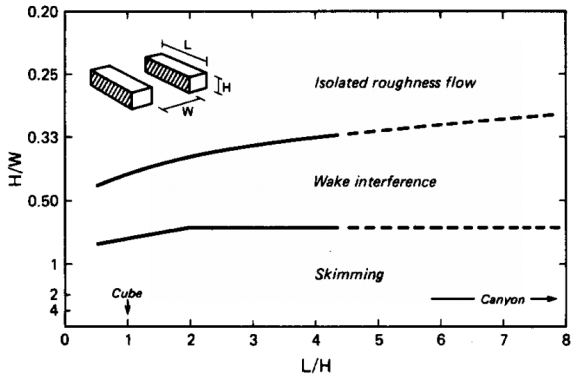

Figure 2.5: H/W and L/H ratios for different flow regimes, from Oke [1988]

The skimming flow (2.4c) occurs when the H/W ratio is so high, that the airflow barely enters the canyon because of a recirculating vortex at the centre of the canyon. Soulhac et al. [2008]

According to Oke [1988], these three type of flows have certain ratio values for which they change. And not only that, also the L/H ratio has effect on the flows. The L/H ratio describes the lengthwise shape of the canyon in relation to the building (long street and tiny houses: >1, short street and tall buildings: <1). Figure 2.5 illustrates these thresholds. Important to note is that for larger values, these thresholds seem to blur more and more, as illustrated by the dotted lines.

Asymmetric canyons, where the two facing buildings have different height, also influence the flow behaviour. According to Park et al. [2019], the taller downwind building increases the pressure and turbulence at the pedestrian level. The flow causes a horseshoe type flow effect that depends on the length of the canyon (fig. 2.7).

2.1.3 Street alignment and intersections

Claus et al. [2011] also look at the influence of wind direction in an idealized building environment, where blocks are arranged in staggered and square arrays. They have found that the average in-canyon wind direction is mostly independent from the prevailing wind direction. In short, this means that the in-canyon flows are guided by the objects.

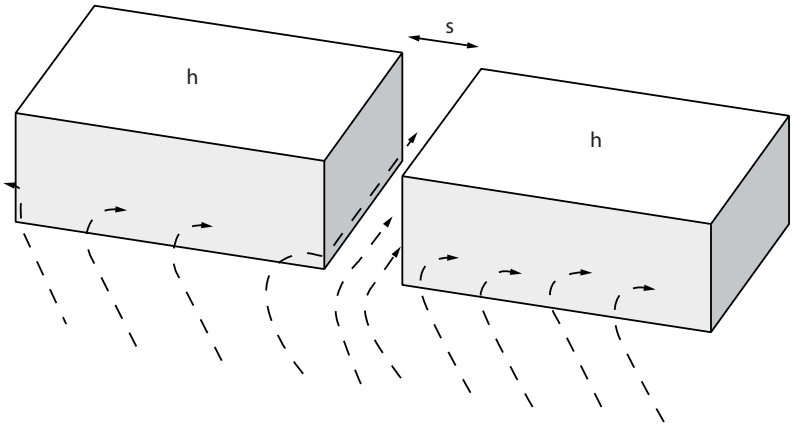

Figure 2.6: Flow pattern at the near-ground level through a gap s between two buildings similar in height, where flow is arriving from an angle. Reproduced from Zajic et al. [2011]

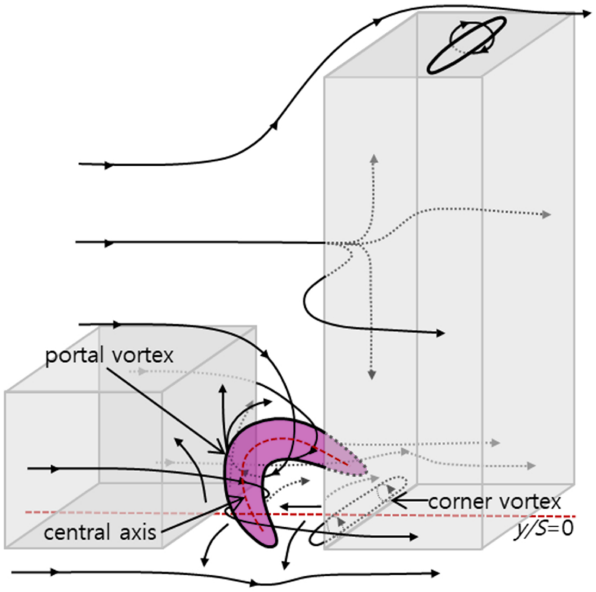

Figure 2.7: The flow in asymmetric canyons with cross wind. Horseshoe flow is illustrated by the purple figure. Adjusted from Park et al. [2019].

Soulhac et al. [2009] investigated the flow and dispersion around street intersections. They mention that even for simple intersection configuration, the flow structure is very complicated and would require many experiments and simulations. Soulhac et al. [2009] used wind tunnel and numerical simulations on simple and idealised intersections to study the wind velocity and pollutant concentration fields as a function of the external wind direction. Soulhac et al. [2009] found that for the wind directions more aligned with the street, the average flow velocity is roughly the same for the entire length of street. However, for wind directions not aligned with the street, the flow velocity inside the canyon is significantly lower compared to the aligned streets.

Illustrated in figure 2.8 are the different flow behaviours in as a result of different wind directions ϕ_c. Visible 2.8a with $\phi_c = 0°$, is the wind flowing uninterrupted from west to east, with vortices at the north and south street entrance. These flow patterns continue to change from a channeling flow towards are helical flow pattern with wind direction changing to $\phi_c = 45°$. These flow patterns are also 3D illustrated in figure 2.9.

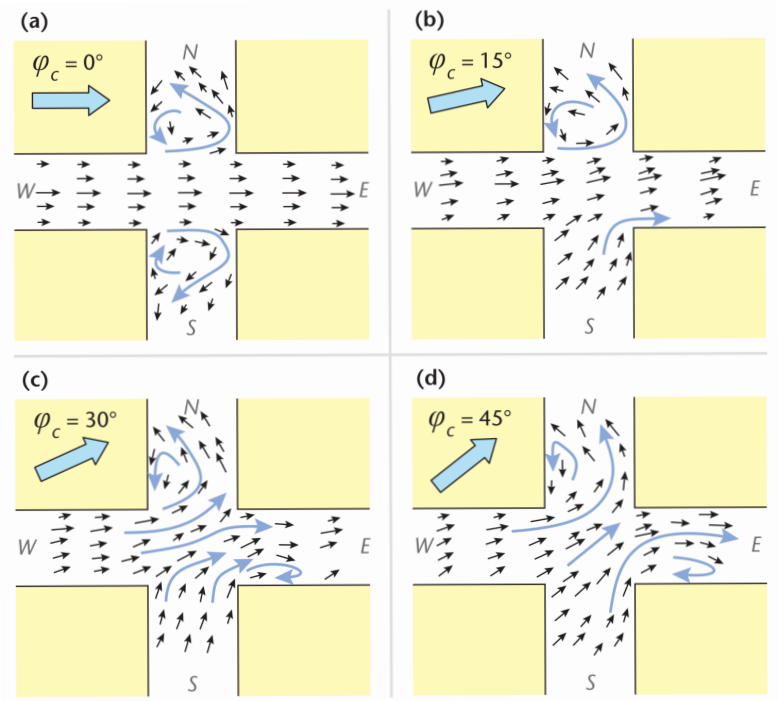

Figure 2.8: Flow behaviour at 4-way street intersections, for different above canyon wind directions. Taken from Oke et al. [2017]

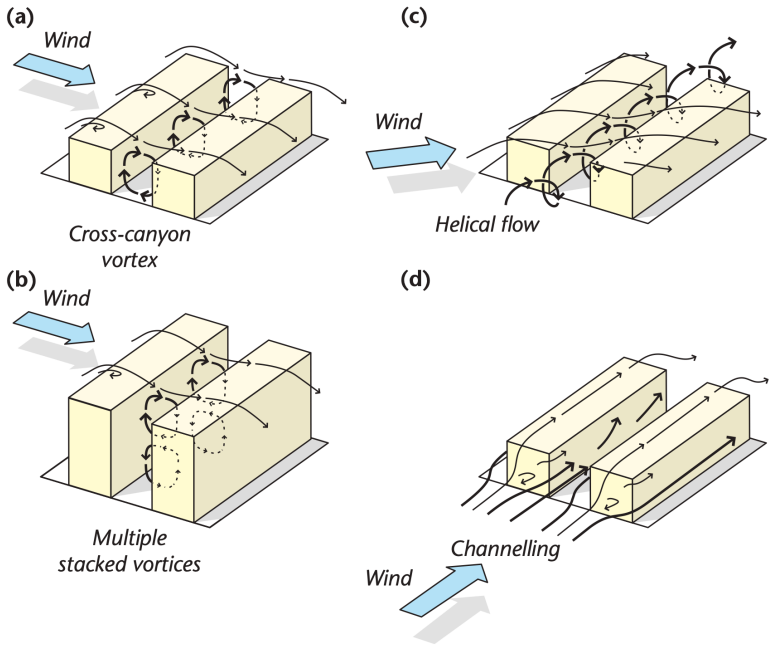

Figure 2.9: Typical flow patterns in the urban canyon: (a) cross-canyon vortex, (b) multiple stacked vortices, (c) helical flow along the canyon and (d) channeling flow along the canyon. Taken from Oke et al. [2017].

2.1.4 Roughness length

Roughness length, z_0 [m], is the main factor in the urban boundary layer describing the materialistic and terrain properties that induce friction and turbulence. For instance, adding tall buildings and large trees to a low-rise building village area, increases the overall roughness of the area Oke [1988]. Additionally, larger z_0 values indicate a greater intensity of turbulence caused by the morphology.

Roughness length z_0 can be determined by measuring the relative change in mean wind velocity (u_1 and u_2) with height (z_1 and z_2) directly above the roughness element where d is displacement length (2.1) [Wieringa, 1992].

$$u_1/u_2 = \ln\left[(z_1 - d)/z_0\right] / \ln\left[(z_2 - d)/z_0\right] \tag{2.1}$$

Or, if multi-level measurements are unavailable, single-level gustiness σ_U can be used for calculation of roughness length (2.2) [Wieringa, 1992].

$$\sigma_{U(Z)}/U_Z \approx 1/\ln(z/z_0) \tag{2.2}$$

Additionally, roughness length can be determined with the use of a reference station, for example located at an airport, by a logarithmic transformation model presented in (2.3) [Wieringa, 1986]. Here, A stands for the local measurement station whereas B stands for the reference station.

$$\bar{u}_{zA} = \bar{u}_{zB}\left[\frac{\ln\left(\frac{z_{\text{ref}}}{z_{0B}}\right)\ln\left(\frac{z_A}{z_{0A}}\right)}{\ln\left(\frac{z_B}{z_{0B}}\right)\ln\left(\frac{z_{\text{ref}}}{z_{0A}}\right)}\right] \quad \left(\text{ms}^{-1}\right) \tag{2.3}$$

However, just as Wieringa [1992] mentions, roughness values are often assigned by visual inspection, photos or land-use maps because local z_0 values are rarely available. For this reason, a categorical roughness length classification, that will be used in this thesis, is introduced by Wieringa [1992] in table 2.1.

2.2 MORPHOLOGICAL ANALYSIS

Morphological analysis is the use of data to provide insight into the urban fabric. Many studies have been done to using urban indicators such as building density [Kubota et al., 2008; Zhang et al., 2020], height variation [Chen et al., 2017], height-to-width ratio [Park et al., 2019; Memon et al., 2010; Razak et al., 2013; Mou et al., 2017; Xie et al., 2007] and street network analysis. In several studies they investigated the relationship between morphology and meteorological conditions, such as temperature, pollution and wind flows [Badach et al., 2020; Samsonov et al., 2015].

Samsonov et al. [2015] computed direction of the canyon using the street network. The same study used a computational method to calculate the height-to-width ratio using a triangular irregular network (TIN), where the non-built space is subdivided in triangles.

2.3 OTHER WIND RELATED PARAMETER OUT-OF-SCOPE

In multiple studies the building density is calculated for an area of interest as indicator to describe building typologies (Kubota et al. [2008]; Tsang et al. [2012]. However, this parameter is considered quite ambiguous, as heterogeneity is always present in the urban form [Berghauser Pont and Haupt, 2009]. As illustrated in

z_0 (m)	Landscape description
1: 0.0002 "Sea"	Open sea or lake (irrespective of the wave size), tidal flat, snow-covered flat plain, featureless desert, tarmac and concrete, with a free fetch of several kilometers.
2: 0.005 "Smooth"	Featureless land surface without any noticeable obstacles and with negligible vegetation; e.g. beaches, pack ice without large ridges, morass, and snow-covered or fallow open country.
3: 0.03 "Open"	Level country with low vegetation (e.g. grass) and isolated obstacles with separations of at least 50 obstacles heights; e.g. grazing land without windbreaks, heather, moor and tundra, runway area of airports.
4: 0.10 "Roughly open"	Cultivated area with regular cover of low crops, or moderately open country with occasional obstacles (e.g. low hedges, single rows of trees, isolated farms) at relative horizontal distances of at least 20 obstacle heights.
5: 0.25 "Rough"	Recently-developed "young" landscape with high crops or cops of varying height, and scattered obstacles (e.g. dense shelterbelts, vineyard) at relative distances of about 15 obstacle heights.
6: 0.5 "Very rough"	"Old" cultivated landscape with many rather large obstacle groups (large farms, clumps of forest) separated by open spaces of about 10 obstacle heights. Also low large vegetation with small interspaces, such as bushland, orchards, young densely-planted forest.
7: 1.0 "Closed"	Landscape totally and quite regularly covered with similar-size large obstacles, with open spaces comparable to the obstacle heights; e.g. mature regular forests, homogeneous cities or villages.
8: $\geq$ 2 "Chaotic"	Centres of large towns with mixture of low-rise and high-rise buildings. Also irregular large forests with many clearings.

Table 2.1: Revised Davenport roughness classification by Wieringa [1992]

figure 2.10, both buildings are different in shape and size, but have the same building density compared to the plot. Additionally, I am looking for parameters that describe certain geometric or morphometric characteristics on a building level scale. As mentioned before, building density is normally calculated for a bigger area, neighborhood or city part. This is why I have decided not to include this parameter in the scope of this thesis.

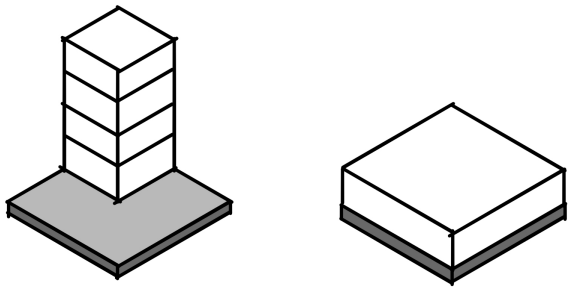

Figure 2.10: Ambiguity of the building density/aspect ratio

Adolphe [2001] proposes several morphological indicator that describe the environmental urban performance on a microscopic level (buildings and building blocks). As an alternative to the well-established H/W ratio, Adolphe [2001] introduces *rugosity*, *porosity* and *sinuosity*. A distinction is made between built and non-built spaces in an area of 400 by 500 meters. This gives the impression that these indicators describe an area, instead of local variable such as street width. Rugosity, for example, is the product of the height of buildings and their area, divided by the total (built and non-built) area.

Additionally, the relation between the performance indicators and wind potential it not researched extensively. Therefore, I have decided not to include these indicators in this thesis.

2.4 METHODS FOR CALCULATING MORPHOLOGICAL PARAMETERS

Badach et al. [2020] calculates the urban canyon parameters in a similar way than the approach used in previous work by Ceccarelli et al. [2019], where every 5 meter the perpendicular distance from the street network to the nearest facade was measured. However, the results are filtered to contain only H/W information of a certain ratio and thus does not provide a continuous map.

Another approach for calculation H/W ratio is described by Jhaldiyal et al. [2018], where a form of ray-casting is used. Multiple lines are cast over the area parallel to the wind direction. The lines cross the building footprints, creating an entry point and exit point. Then, the distance between the exit point of one building and the entry point of the facing building is used to estimate street width. This approach is quite interesting, because the approach uses the wind direction to calculate a relative street width.

VD have also been used for urban analysis [Roberts et al., 2005; Fleischmann et al., 2020; Ceccarelli et al., 2019]. A VD is a mathematical partition (or tessellation) of space into cells (or regions). The edges of every cell are defined by the Euclidean distance of every vertex in a set of vertices, defined in $\mathbb{R}^2$, where the edge is of equal distance to two vertices (fig. 2.11a). It can be described formally by:

$$\mathcal{V}_p = \left\{ x \in \mathbb{R}^2 \mid \|x - p\| \leq \|x - q\|, \forall q \in S \right\} \tag{2.4}$$

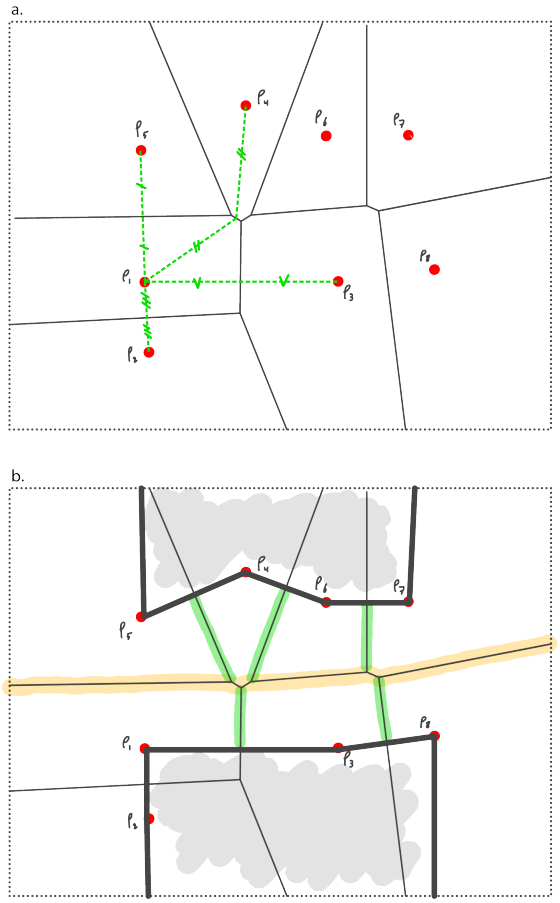

Figure 2.11: a. input points for VD, where the VCs are constructed by Euclidean distances between points, b. when overlaying the building footprint, the edges (green) toward the street center (yellow) can be computed

VDs have been used in street centerline reconstruction as a medial axis calculation (Roberts et al. [2005]). This is done by the equal distance property of the VD. When using the building's geometry as input vertices for the VD, the VCs meet in the middle for buildings facing each other (fig. 2.11b). The in-common edges between the buildings, representing the equal distance to the vertices, can then be used as the street's centerline. This is illustrated by the yellow line in figure 2.11b.

VD are also being used for urban morphological analysis with different purposes, as Fleischmann et al. [2020] mention in their research. The python library momepy is a result of this research. Momepy also uses VD in its algorithm for the analysis of morphological parameters. It groups the cells on building id to reduce the overall amount of cells and edges. This results in a voronoi tesselation which no longer can be used to determine street widths in the way this thesis requires. Additionally, it loses a lot of information, especially the facade to street relationship.

Samsonov et al. [2015] used a TIN method of calculating the street widths, or more accurately: the inverse of VD, Delaunay triangulation (DT). From the resulting triangulation, for every triangle, it uses the altitude perpendicular to the triangle side not intersected by the street network line to measure street widths. Thus, this method depends on a street network dataset to work. Additionally, Samsonov et al. [2015] have chosen not to calculate street widths for the space not classified as to what they call *directed canyons*.

3 METHODOLOGIES

The contents of this chapter describe the workflow and the design process of various algorithms used in the calculation of the morphological parameters. First, I introduce the research area and meteorological station in §3.1. I move on the explain the input datasets and tools used in this thesis (§3.2). After, I describe in-depth the different methodologies to compute the morphological parameters (§3.3 - 3.7). Finally, I elaborate on the scoring system for potential increase in wind velocity in §3.8 and validation of the score using meteorological data in §3.9.

3.1 RESEARCH AREA AND METEOROLOGICAL STATIONS

In this thesis, an area of Rotterdam and Schiedam is selected as research area. The area covers about 9,2 km² and spans from Rotterdam Central Station to Schiedam Central station, down to the Nieuwe Maas river (fig. 3.1c).

The area has been selected due to the presence of different typologies, including an industrial zone (e.g. Nieuw-Mathenesse), high-rise buildings (e.g. Centrum), squares (e.g. Heemraadsplein) and waterways (e.g. Coolhaven) which makes it a good area for testing different methodologies.

Additionally, meteorological data for two locations in the area of interest is available through the RainGain project of TU Delft and can be accessed on weather.tudelft.nl. One station was located in Centrum, near the Central Station, which recorded meteorological data from April 2013 till November 2014 (fig. 3.1a). The second weather station is located at Delfshaven and has been recording data since April 2015 (fig. 3.1b). The dataset contains 5-minute average measurements.

Two meteorological stations outside of Rotterdam are to be used as reference stations. One station is located at Rotterdam / The Hague airport and data is made available by Koninklijk Nederlands Meteorologisch Instituut (KNMI) (Royal Dutch Meoterological Institute), specifically through wow.knmi.nl (accessed: 16-02-2021). It is free of any objects in radius of 100 meters and the station is located 10 meters above ground. The dataset contains 10-minute average meteorological measurements, from December 2018 till January 2021.

The second reference station was located in Oude Leden, placed directly on a grass field, free of any objects. It recorded 5-minute average meteorological data, from April 2013 till December 2015.

Figure 3.2 shows the available meteorological stations and the corresponding time windows between urban stations [left] and the rural reference station [right]. Firstly, immediately noticeable in the figure are the reduced wind speeds that happen in the city (3.2a, 3.2c and 3.2e) compared to the rural reference stations (3.2b, 3.2d and 3.2f).

Secondly, when comparing the urban stations with the reference stations, the urban stations seem to have a more predominant wind direction compared to the more evenly distributed reference stations. The central station (3.2a) wind direction window WSW of [236,25 to 258,75] contains 22.1% of all measurements and close to none measurements from WNW to ENE. This could be explained by the location of the central station station: located close to the facade of a building with an azimuth of 17 degrees, which corresponds to a wind direction of 253 degrees.

(a) Centrum meteorological station placement, from weather.tudelft.nl

(b) Delfshaven meteorological station placement, from weather.tudelft.nl

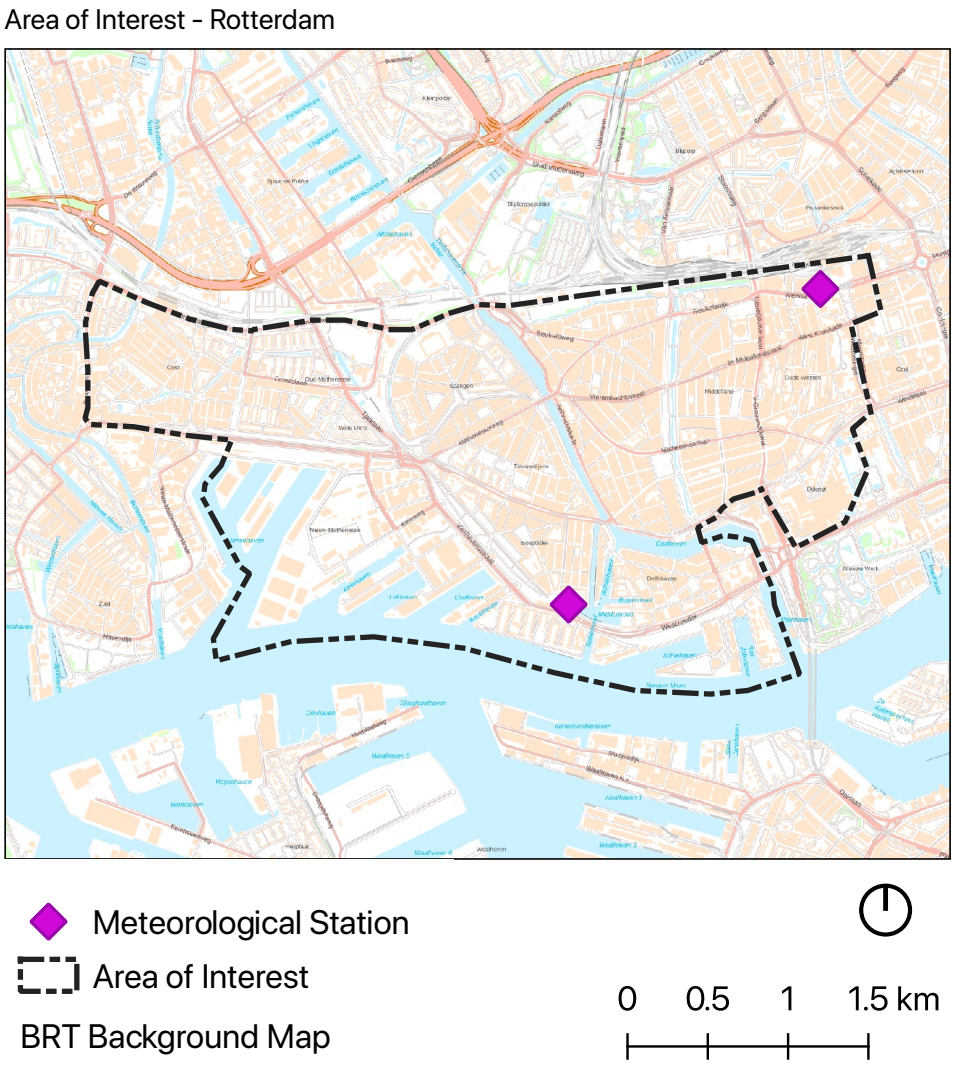

(c) Rotterdam and Schiedam area of interest and meteorological station locations.

Figure 3.1: Placement of the two meteorological station in the area of interest

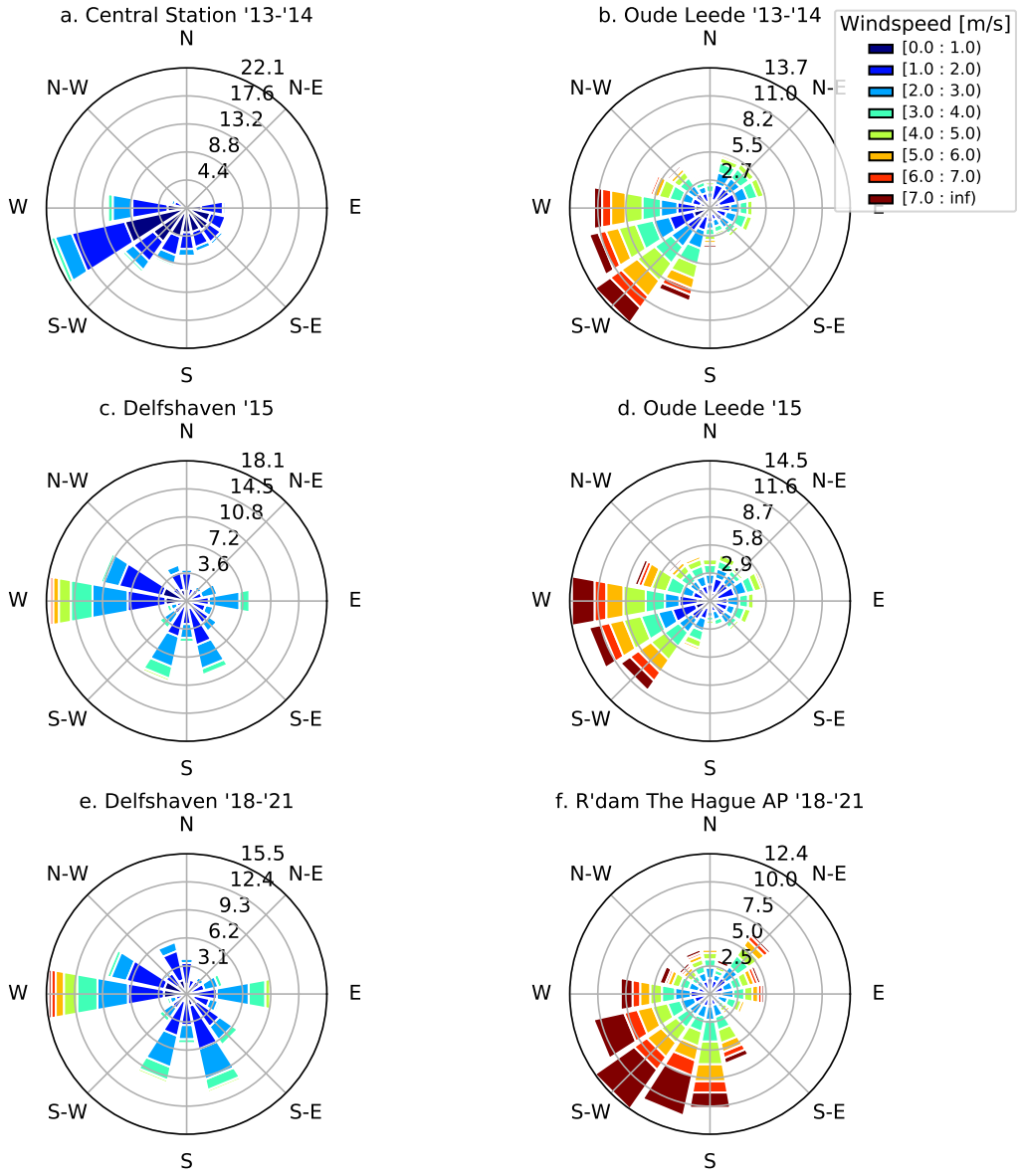

Figure 3.2: Windrose plots with available data in the area of interest for the urban stations [left] and reference stations [right] at corresponding time frames

The Delfshaven station has a predominant wind window, West of [258,75 to 281,25], that remains roughly the same in two different time windows (3.2c and 3.2e) even though the distributions of the two reference stations (3.2d and 3.2f) are different. Even more noticeable is the absence of WSW and SW wind direction in both 3.2c and 3.2e. Upon inspection of satellite images, this could be explained by four tall trees and a tall building possibly blocking the wind coming from these directions (3.3).

Thirdly, higher wind speeds are measured at the reference stations than at the urban stations. This shows that the urban environment drastically affects wind speeds. But also, that some wind directions have increased potential for higher wind velocities.

Figure 3.3: Situation around the Delfshaven meteorological station with tall objects

3.2 THE CHOICE OF INPUT DATASETS AND TOOLS

For this thesis, the input datasets consist of data from the Basisregistratie Adressen en Gebouwen (BAG) regarding the building footprints, Centraal Bureau voor de Statistiek (CBS) for neighbourhood polygons and Algemeen Hoogtebestand Nederland (AHN) 3 for building height information. All three datasets are publicly available through the Publieke Dienstverlening Op de Kaart (PDOK)[1] Application Programming Interface (API) plugin, making it easy to download and use. Also, for any data analyst the quality of the input datasets are essential: trash in equals trash out. The BAG dataset is regularly updated by the municipality to be up-to-date. The AHN3 height dataset done using LiDAR technology is an improvement on AHN2 with better precision, higher accuracy and increased point density. The BAG building dataset has been enriched with the AHN3 height information to create a combined 2.5D dataset, also described as Level of Detail 1 (LoD1) where building footprint are pulled up to the building height to create blocks with flat roof structures. This process is done by the 3D geoinformation research group of TU Delft (Faculty of Architecture and the Built Environment). The dataset is accessible through Web Feature Service (WFS)[2].

Additionally, the Basis Grootschalige Topografie (BGT) dataset is used for classifying the open space (non-built) typologies and materials, such as water bodies, vegetation and pavement for determining roughness length.

All of the before mentioned datasets are stored in a PostgreSQL database with PostGIS extension to be able to handle the geometries. This workflow is easy and intuitive to work with, as data is easily extracted from the PDOK API plugin within QGIS 3.10 and stored in a local database. It also allows me to easily bring the data into my Python environment using a PostgreSQL connection. All algorithms are written in Python 3.7 using various libraries such as Shapely, GeoPandas and SciPy. And finally, I use QGIS 3.10 to perform and inspect the output of various algorithms. QGIS is a free and open source geographical information system (GIS) that I use to manage, process, analyse and present geo-information. Beside QGIS, all tools and datasets discussed here are open, freely accessible for (re-)use.

1 https://www.pdok.nl
2 https://3dbag.nl/nl/download

3.3 DETECTING TALL BUILDINGS

I would be wrong to say that building the query for Tall Buildings is a difficult challenge. A simple WHERE statement combined with a threshold height would give me the result I need. However, the thought process behind the query is a bit more complex. As a 'tall' building is relative to its environment, it is hard to clearly state what to consider a tall building: a 70 meter building next to the Burj Khalifa (828m), might not be considered tall. The Dutch government classifies buildings with a height exceeding 70 meters as a tall building. This, however, is mainly based on the fire safety demands by the Bouwbesluit laws (article 2.14) [Rijksoverheid, 2021]. The 70 meter is a good starting point, but again does not provide a good method for indicating tall buildings. And so this calls for another approach to the tall building methodology, one that takes into account the average building height of all buildings inside a certain area of interest, the standard deviation of these building heights and the 70 meter threshold.

For this thesis, I analyzed the heights of all buildings in the area of interest by looking at the histogram and the probability density function of the building heights (fig. 3.4). The histogram shows a positively skewed distribution of building heights. A maximum building height of 172 meters. An average of 11 meters (3 story) buildings with a standard deviation of 6 meters. The 70 meter threshold is not realistic in this case, as there are only 8 buildings out of 18400 in the area that exceed this threshold.

Consequently, I chose a threshold of 23 meters (which would correspond to a 6 or 7 story building) based on the average of and 2 times the standard deviation. As visible in figure 3.4, the 23 meter threshold falls within the upper whisker. Also noticeable, are the high amount of outlier values in the boxplot.

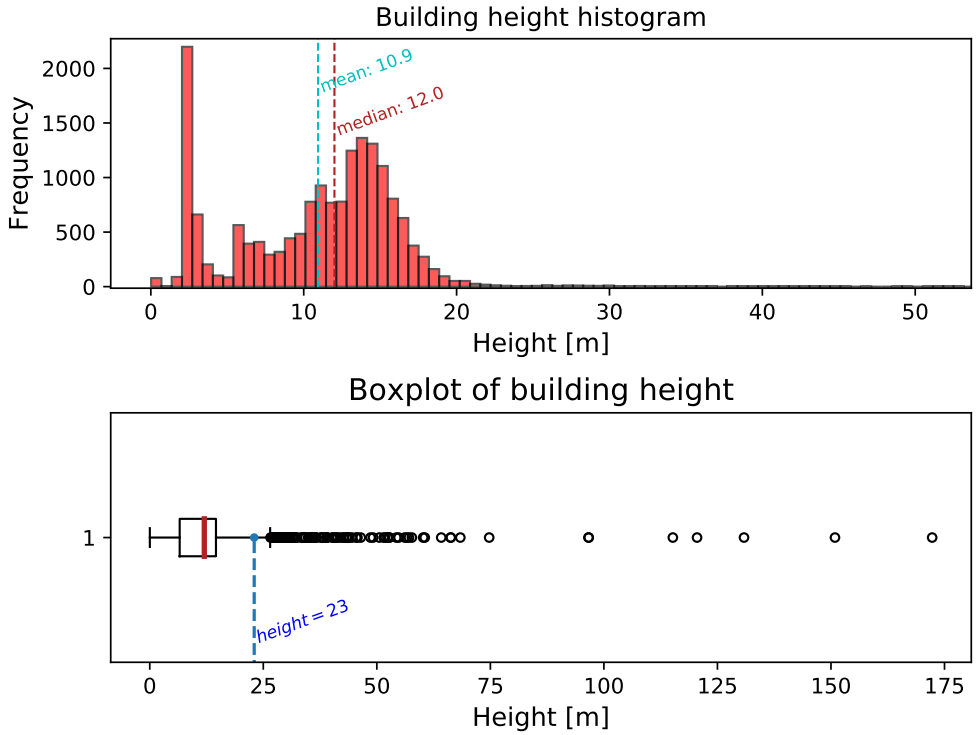

Figure 3.4: Top: histogram showing the distribution of building heights, Bottom: boxplot of building height, with horizontal line for building height equals 23.

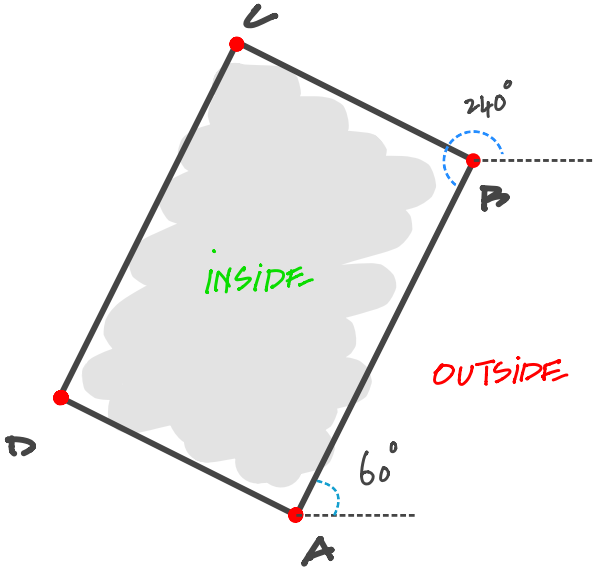

Figure 3.5: Rectangle *R* explained

3.4 ANALYSING WIND- AND LEEWARD FACADES

This methodology looks at individual buildings, and determines which parts of the facades are wind- or leeward sides based on the given wind direction. It does so by exploding (or breaking down) the 2D footprint of the building into its separate line segments. E.g. rectangle *R* into line segments AB, BC, CD and DA (fig. 3.5). Then, for each line segment the azimuth is computed and compared to the wind direction using trigonometry.

Before exploding, I do a check to see if the building footprint is organised counter-clock wise. If the vertices are all organised in the same way, the azimuth of the line indicates which side of the line is inside, and which side of the line is outside (or facade).

To illustrate this, consider the following: a rectangle *R* is defined by vertices ABCDA, organised counter-clockwise (fig. 3.5). It is clear to us, that the inside of *R* is left of each line segment (AB, BC, CD, DA). If we were to change to orientation of *R* to ADCBA and still assume that the left of each line segment is inside, we would misinterpret *R* because left of AD is now outside of *R*.

Likewise, the organisation of the vertices also influence the azimuth of each line segment of *R*. Azimuth is the angle between a reference line and the line itself. Consider that the azimuth of line AB is 60 degrees when *R* is organised CCW. The flipped organisation of *R*, CW, the same line segment (now BA), would have an azimuth of 240 degrees.

To determine which facade is wind- or leeward, I make use of these two principles. Using the orientation of the geometry I establish the outside of every line. Then, I compare the azimuth of the line with the wind direction to classify the lines as wind- or leeward.

After calculating the wind- or leeward attribute of every facade, I calculate the angle of attack (AOA) between the facade and the wind direction parameter. It does so for every facade, both wind- and leeward, so that in I can calculate and visualise how streets line up with the wind direction. More detailed explanation of the calculation of AOA will be provided in §4.4.

This reason for using this methodology for calculating wind- and leeward sides and AOA, is because it makes use of the polygon's own characteristics and basic trigonometry. And so by keeping the methodology simple, the computation time needed for all buildings in the 9,2 km² area stays to a minimum.

It should be noted that this methodology does not take blocked facades into account. Shared walls between buildings are not considered, as it merely looks at the individual building footprint. In order to deal with this, the footprints are merged into building blocks to remove any shared walls so that only the outer shell is left.

3.5 USING VORONOI DIAGRAMS FOR STREET WIDTHS

In the research done by Ceccarelli et al. [2019], four different approaches were used in order to calculate street width. The input to the approaches were 2.5D building footprints and a road network. The street width relies on the distance between the individual building facing the road segment. This relationship describing which building is facing the street is established by means of a VD.

I decided not use the road network, because of the chaotic nature of the urban environment and the dataset: sometimes multiple lines in a two way street, intersections and other anomalies. But most important, is that the street network limits the area of investigation to just streets and not spaces where streets are not present e.g. water surfaces, backyards or parks. Instead the urban space (non-built area) is divided into VCs which are constructed using points from discretised building footprints. Discretising footprints is done by dividing the individual lines into points.

Subsequently, the descrised footprint points are used as an input for the VD. The VD in this thesis is calculated using the pyhull library. This library takes as input a list of points and creates the diagram. In the calculation of the VD, some vertices go to 'infinity' because they are not bounded, and are instead given coordinate values of -10.101. These cells should be filtered out. A way to do this, is by using a discretised polygon as the bounding box and removing all cells that lie outside this box in the result. I am using the neighborhood polygon from CBS as my bounding box (fig. 3.6).

Unfortunately, the pyhull library only uses simple points without any attributes. Meaning that the VCs in the diagram lose their relationship with their corresponding building. To reinstate this relationship, another operation is done which adds the building identifier to the Voronoi cell (VC) if they intersect. This operation makes it possible to relate the morphological parameters to both the buildings and the cells.

Beside using the VD for calculating street widths, the diagram is also a useful for partitioning the non-built areas. The VD is used as the background map for the morphological attributes, where every VC is assigned these attributes. VCs that do not have a building attached to it will not receive these attributes, as the UC parameters depend on building geometry.

3.6 DETERMINING STREET LENGTHS

The method to determine the length of an urban canyon was not done in previous research. There was no existing method. Using the length of a street segment is not a clear representation of an urban canyon. Because the urban canyon is the space between buildings or facades (built), regardless of the situation such as road, water or 'empty space' (non-built). Therefore, it made no sense to actually use the road network dataset, as done by Ceccarelli et al. [2019]; Badach et al. [2020]; Samsonov et al. [2015], because I would be limiting the methodology to classified roads.

So far, most of the methods discussed in urban canyon calculation ([Ceccarelli et al., 2019; Badach et al., 2020; Samsonov et al., 2015]) relied on the street network lengths. Because of the design criteria (not using street networks) a new methodology is proposed in this thesis. Before that, I will first explain why the street network is an insufficient method for calculating canyon lengths.

Figure 3.6: The neighboorhood polygon as bounding box for creating a subset of the total Voronoi diagram

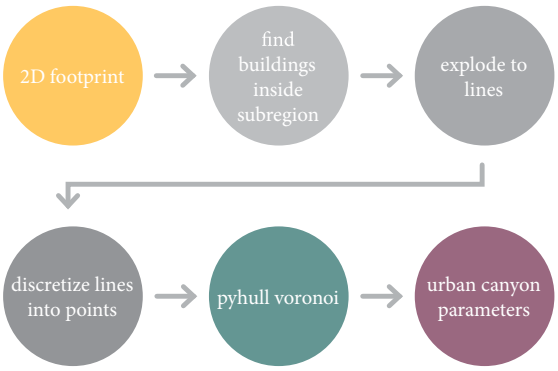

Figure 3.7: Workflow for creating the Voronoi diagram

Figure 3.8 illustrates several reasons not to use the street network. In the top left image, the street segment turns a corner. As shown in §2.1.3, depending on the wind direction and the azimuth of the street, wind flow through the canyon differently. This segment should then be split according to the azimuth of the lines. But this raises other problems, such as: where, how and when to split the segment.

Figure 2.8 also demonstrated that the canyon starts at the edge of the building. In the top left figure of 3.8, the line starts right in the middle of the intersection and therefore not representing the actual length of the canyon.

Additionally in the top left and the top right figure of 3.8, there are gaps present between the buildings facing the street segment. These gaps also cause wind flow to behave differently (§2.1.2), and should be taken into account when measuring canyon length. Furthermore, in the top right figure four lines with differently placed vertices are used to represent streets in the non-built area. This poses a problem not only for the creation of the VD, but also simply: what road should be classified? This 'chaotic' nature of the built environment makes it complex and hard to find a simple solution that can be translated into an algorithm.

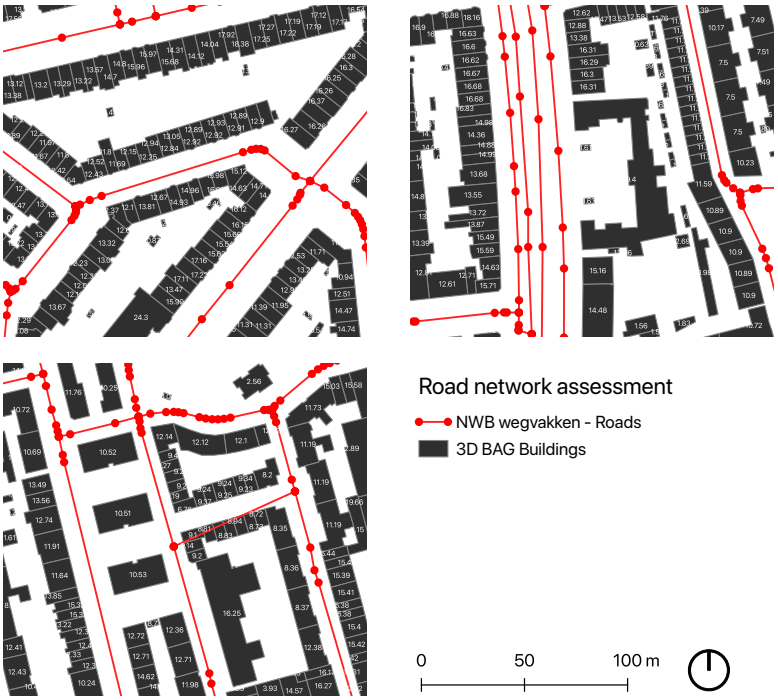

Figure 3.8: Illustrating the various reasons of not using the National Road Network dataset for calculating canyon lengths.

Two more reasons for not using the road network dataset, are illustrated in the bottom left figure of 3.8. Most obvious, there is a road segment going straight through the buildings, making it impossible to determine street width. Secondly, and this illustrates the limiting factor of using the street network, there are no lines between the rectangular buildings with height 10.52, 10.51 and 10.53. If a the road network was used, these buildings will not be considered as an canyon. This is problematic, because these standalone buildings do have an impact on the wind patterns around them and create a canyon between the buildings.

To conclude, it is not the length of the street that matters to the wind flow, but the length of the objects. Which, in turn, results in the length of the total continuous facade of a side of the building block. This also means that the gaps in the building block's facade control the length of the canyon. Additionally, the direction of the canyon might also determine the canyon length.

The new method will use the merged building footprints (or building blocks). This allows for the calculation of the length of the entire block representing the canyon. Using the footprint of the building block, every individual line is classified based on the azimuth of itself and the lines prior. This way, both the gaps and the change of direction in the canyon are considered.

To add the canyon length property to the VD, the individual lines are grouped and the total length is measured to establish to continuous facade length. After, the length property is assigned to the overlapping VC.

3.7 DETERMINING ROUGHNESS LENGTHS FOR NON-BUILT AREA

There are several ways of calculating and assigning the roughness length z_0 values, discussed in §2.1.4. Since there are no z_0 available for the area of interest, I will use the third approach discussed in §2.1.4. This approach relies on assigning the z_0 value based on land-use maps. The BGT dataset contains polygons dividing

the non-built area (e.g. roadparts, vegetation, un-vegetated areas and waterparts), with additional attributes describing their material properties. Using table 2.1, it is possible to match these material properties to their respective z_0 value, shown in 3.1. Then, the z_0 value should be added to the VD base map, where every VC is assigned the correct z_0 value.

3.8 SCORING THE VORONOI CELLS FOR WIND POTENTIAL

After the calculation of all the parameter mentioned in this chapter, I end up with a classified VD. Every VC contains the attribute of the related building height, canyon width and length, wind- or leeward property of the facade for certain wind directions, the AOA between the facade and the wind direction and a roughness length z_0 value. Next, I will need to translate these parameters into potential wind velocity increase. However, there is no current methodology how to do this, as the relationship between the morphological parameters and wind potential is not clearly described. Therefore, I propose a simple method of scoring the parameters based on threshold values. The scoring system is illustrated in table 3.2, where every parameter has been given thresholds that correspond to a score from 1 to 5 (building height, H/W, AOA, z_0), 1 to 3 (W/L, L/H) or 1 or 2 (windward).

There is certain overlap between parameters, such as H/W and building height. However, the building height and the H/W ratio (describing the cross-section shape of the canyon) both have a significant impact on wind flows in the urban environment and are thus both present in the scoring system. Additionally, the H/W ratio does not immediately indicate the presence of a tall building, as the building height is divided by canyon width.

3.9 ANALYSING THE METEOROLOGICAL DATA

As mentioned in §3.1, there are two meteorological stations in the research area. This is limits the validation, as this only allows me to measure wind speed and direction for two particular spots in an area of 9,2 km^2. Knowing this limitation, I will still try to validate the results of the score system. The data comparison will be done using Python, with the use of libraries such as Pandas, Matplotlib and Seaborn.

For the validation, I will look at the certain wind speeds and direction from data gathered at the reference stations, and compare them with the measurements at the urban station at the same moment in time. Beside wind speed and direction, the meteorological stations from the TU Delft also measure temperature and relative humidity. And for the validation, the time of day or night and seasonal behaviour should be taken into account for the comparison.

type	z_0
traffic area	
closed pavement	0.005
semi closed pavement	0.005
open pavement	0.005
plant cover	
grass and herbs	0.03
plants and roses	0.10
shrubbery	0.25
tree area	0.5
unknown	none
unvegetated area	
private property	1
closed pavement	0.005
semi closed pavement	0.005
open pavement	0.005
unpaved	0.03
waterpart	
waterplane, waterway or ditch	0,0002

Table 3.1: BGT layers and subclasses with their respective roughness length values

parameter/score	5	4	3	2	1
building height (H)	$H >= 23$	$15.7 <= H < 23$	$13.34 <= H < 15.7$	$10.3 <= H < 13.34$	$H < 10.3$
H / W ratio (H/W)	$HW <= 0.05$	$0.05 < HW <= 0.4$	$0.4 < HW <= 0.65$	$0.65 < HW <= 1$	$HW > 1$
W / L ratio (WL)			$WL <= 0.07$	$0.07 < WL <= 0.56$	$WL > 0.56$
L / H ratio (LH)			$LH >= 3.69$	$1.42 <= LH < 3.69$	$LH < 1.42$
angle of attack (AoA)	$AoA < 18$	$18 <= AoA < 36$	$36 <= AoA < 54$	$54 <= AoA < 72$	$72 <= AoA <= 90$
windward				*Yes*	*No*
roughness length (z_0)	0.0002	0.005	0.03	0.1	$z0 <= 0.25$

Table 3.2: Thresholds for different scores, thresholds adapted from Oke [1988]; Wieringa [1992]; Tsang et al. [2012]

4 IMPLEMENTATION

This chapter contains the implementation of the different methodologies presented in chapter 3. Also, the algorithms are presented in (simplified) pseudo-code. The code is published on GitHub through https://github.com/CodeWessel/windystreet.

4.1 CREATING THE VORONOI DIAGRAM

The Algorithm 4.1 is the implementation of the voronoi diagram. The result is a VD that can be used as a base map. The morphological parameters will be added to every VC as an attribute.

Algorithm 4.1: VORONOI (VD)

Input: 2.5D polygons of building footprints P_b
2D polygons of neighborhood P_n
Output: Voronoi diagram VD

```
P_b, P_n ← get footprints from SQL Database
for i in P_n do
    get P_b i within P_n i
    discretize P_b i and P_n i into equidistant Points p_b, p_n i
    create VDi with p_b, p_n i using Pyhull Voronoi
    remove cells with vertices to infinity (or −10.101)
    add VDi to final VD
```

The limitation of this algorithm lies in the use of the neighborhood polygon. Because I have used the buildings that fully lie within the neighborhood polygon, the buildings that intersect the edge are not considered in the VD. For these buildings, no canyon width or height calculation is done. Additionally, the neighborhood polygon is also added to the VD. The VCs that originate from the neighborhood polygon are not considered for the canyon height and width implementations.

4.2 CALCULATING CANYON HEIGHT AND WIDTH

Using the VD from §4.1, we can begin to calculate the canyon widths. This is done using Algorithm 4.2. Here, for every building, the intersecting VCs and edges are found. Then, using overlay difference, the building polygon area is subtracted from the edge. This results in a line that starts at the building edge towards the (presumed) center of the canyon (fig. 4.1).

The length of the edge is measured and added to the VC to which the edges belongs. The edges of the VC can intersect the building twice, and so the average of the edge lengths are taken to represent the canyon width for that VC. Additionally, the height attribute of the building that intersected with the VC is also added to the VC. If multiple buildings intersect a VC, the average is taken to represent canyon height for that particular VC.

Algorithm 4.2: CANYON HEIGHT AND WIDTH (VD, P_b, P_n)

Input: Voronoi diagram classified with neighborhoods VD_n
2.5D polygons of building footprints P_b with height attribute h
2D polygons of neighborhood P_n
Output: Height and width enriched Voronoi diagram VD_{HW}

```
1 subset ← get P_b within P_n
2 for region in VD_n do
3     get VD_n cells C within region
4     explode C into edges e
5     for P_b in subset do
6         get e, C intersecting P_b
7         append h from P_b to C for VD_H
8         width w ← overlay difference e with P_b
9         append w to C for VD_HW
```

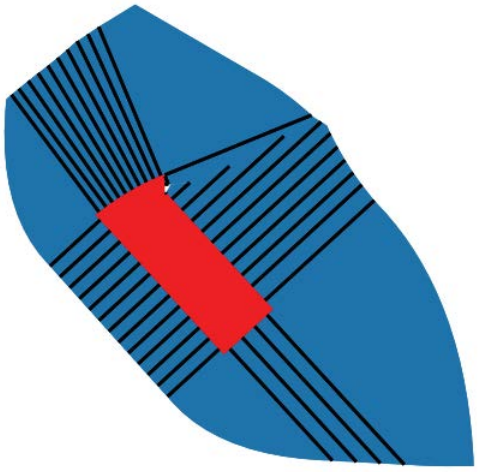

Figure 4.1: Sub-result (line 6 of Algorithm 4.2) showing the intersecting edges (black lines) between the Voronoi cells (blue polygons) and the building (red polygon)

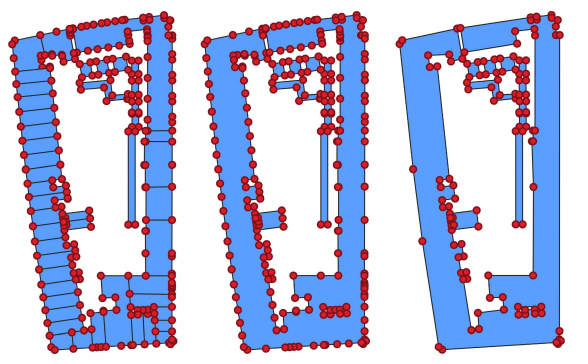

Figure 4.2: Merging the single buildings into block and simplifying the geometry

4.3 CALCULATING CANYON LENGTH

The building dataset contains only polygons of single buildings, not building blocks (or groups) that can be used to compute the 'total object facade length.' To achieve this, the building footprints are merged into one block polygon. Then, the geometry is simplified to remove any unnecessary points. This process is illustrated in figure 4.2. The merging of footprints is done using Boolean operation ST_Union in SQL with a Postgis extension. The simplification is done using Douglas-Pecker algorithm in QGIS3.

With the simplified building blocks, I explode the footprints to single lines to compute the azimuth. A separate function is written for the azimuth calculation, as it is needed for multiple algorithms.

The azimuth algorithm takes the input polygon and explodes it into its separate lines. Then, the start and end points $S_{x,y}, E_{x,y}$ of the line are input for atan2 function that calculates the angle θ between the line and the positive x-axis.

Algorithm 4.3: DETERMINEAZIMUTH (P)

Input: polygon P lines l
Output: polygon P with lines l and azimuth θ

```
if P ← CW then
    flip P to CCW ;
else
    for l in P do
        l_S, l_E ← startPoint S, endPoint E ;
        θ ← arctan2(l_E y − l_S y, l_E x − l_S x)
```

Next, for every footprint line, the algorithm compares the azimuths of the previous 4 lines with the current footprint line. If there is a previous line within a 20 degree threshold, they receive the same group identifier and the length of the line is added to the group. In the end, I reiterate over the entire dataset to append the correct total group length to all grouped lines.

This is illustrated in figure 4.3 where, even with the facade setbacks, the entire length of the south-west facade is classified as group 4, brown.

This methodology is a trial, and improvements can be made by adding more constrains. For example, by also looking at the length of previous lines you could determine if the facade does not have a too big of a setback in the facade. Then, if the setback supersedes a threshold length, it is no longer grouped.

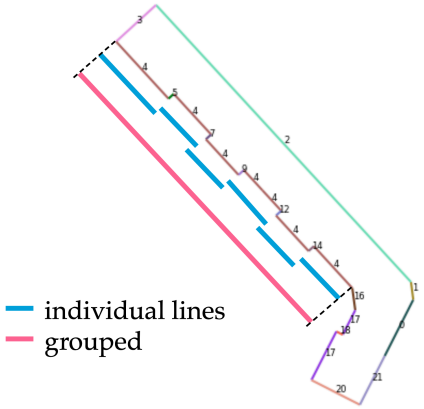

Figure 4.3: Classifying the lines of the building block footprint where individual lines are grouped if lines have similar azimuth.

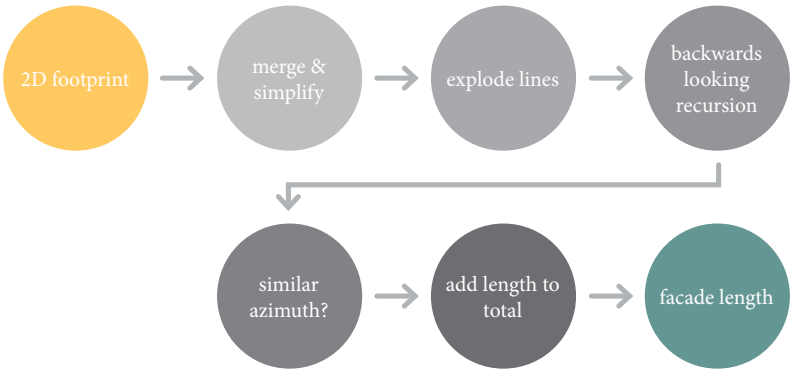

Figure 4.4: Workflow of calculating consecutive facade length

Algorithm 4.4: CANYON LENGTH (P_{block}, VD)

Input: polygon of building blocks P_{block},
voronoi diagram VD
Output: voronoi diagram enriched with canyon length VD_L

$P_{block} \leftarrow$ get block footprints from SQL database
max_backward $\leftarrow 3$
max_azimuth_difference $\leftarrow 20°$
for line f **in** P_{block} **do**
    calculate azimuth θ
    for previous_line $f_p \leftarrow 0$ **to** max_backward **do**
        if $f\theta$ between $f_p\theta \pm max\_azimuth\_difference$ **then**
            group $\leftarrow$ line to previous_line
for *group* ***in*** P_{block} **do**
    calculate group_length $l \rightarrow P_{block}l$
$VD_L \leftarrow$ intersect $P_{block}l$ with VD
write VD_L to SQL database

4.4 CALCULATING WINDWARD AND ANGLE OF ATTACK

The calculation of windward facades and the AOA is done in the same algorithm, as they require the same input data and approach. The counter-clockwise check has already been done in Algorithm 4.4, therefore it is not included in Algorithm 4.5 but is nonetheless important for this algorithm to work as intended.

The windward and AOA algorithm starts with the calculation the azimuth θ (Algorithm 4.3) for every line segment in the building block polygons, mentioned in §4.3. Next, the azimuth of every line is compared with the wind direction parameter to determine if the line is wind- or leeward (fig. 4.5). The result is illustrated in figure 4.6. After, the AOA for the same line computed and converted to the smallest possible angle (fig. 4.7).

The algorithm is run 12 times, for wind direction 0, 30, 60, ... to 330. The output is a dataset with the windward and AOA attribute for 12 wind directions, for every line in every building block. Next, the attributes are added to the VD using QGIS3 vector tool *Extract by Location*. This add the windward and AOA properties to the intersecting VC.

It should be considered that wind direction generally uses the compass rose for denoting degrees, where North equals 0° and East equals 90° (clockwise). Azimuth calculation uses the angle between the facade and the positive x-axis, meaning that East equals 0° and North equals 90° (counterclockwise). To switch between compass rose and azimuth, I use the equation 4.1 for conversion.

$$compass = (450 - azimuth) \mod 360 \tag{4.1}$$

Algorithm 4.5: WINDWARD_AOA (P_{block}, VD, WD)

Input: polygon of building blocks P_{block},
voronoi diagram VD,
wind direction WD
Output: voronoi diagram with cells containing windward and AOA attribute VD_{ww+aoa}

```
for line f in P_block do
    calculate azimuth θ
    if θ ≤ WD < (θ + 180) then
        f_ww ← 1
    else
        f_ww ← 0
    f_aoa ← absolute(WD − θ)
    if f_aoa > 90 then
        f_aoa ← absolute(f_aoa − 180)
VD_ww+aoa ← intersect P_block, f_ww+aoa with VD
write VD_ww+aoa to SQL database
```

4.5 CLASSIFYING ROUGHNESS LENGTH

For this implementation, I make use of the BGT dataset. The dataset contains polygons, classified in several the sub-layers with material properties, shown in table 3.1. The polygons are copied to separate z_0 layers based on their material properties. To add the z_0 value to the VD, the implementation uses QGIS function Overlap Analysis (fig. 4.8). The function takes as input: *1)* the VD base map (geometry type:

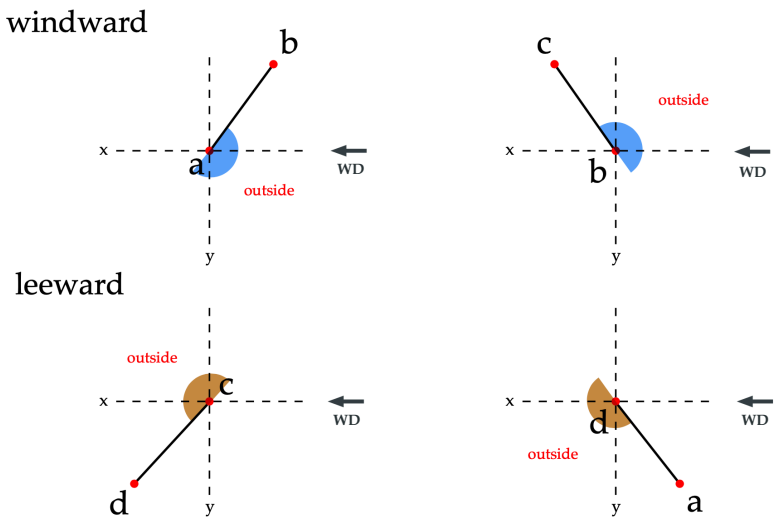

Figure 4.5: Calculation principle of determining wind- or leeward sides with a wind direction of 90 degrees compass.

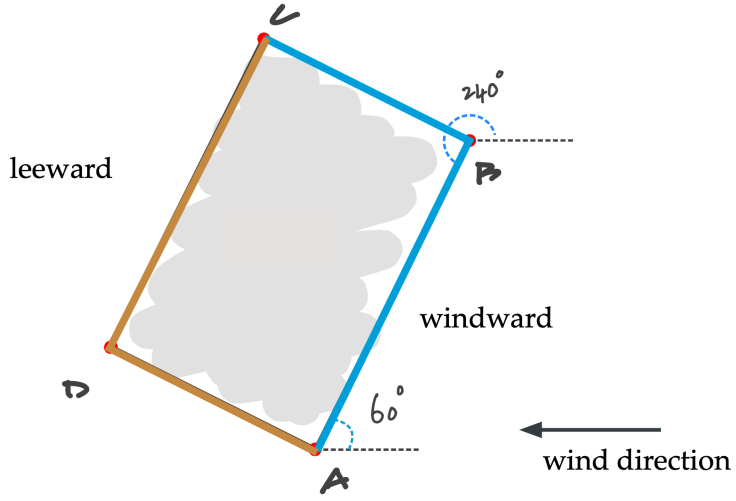

Figure 4.6: Rectangle R wind- and leeward sides caused by wind direction of 90 degrees compass

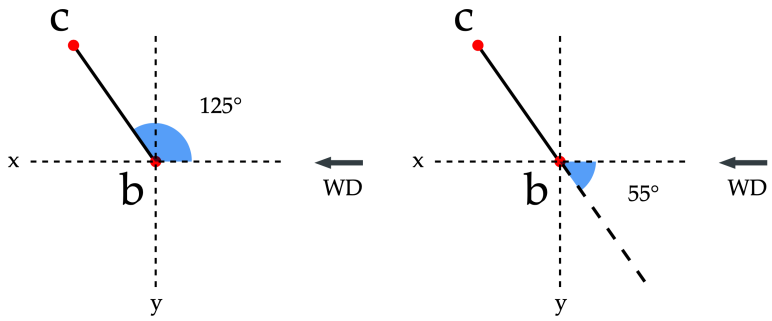

Figure 4.7: Larger angle of attack (left) is converted to smallest angle of attack (right), with a wind direction of 90° compass

parameter	value	score
canyon height [m]	39	5
H/W ratio	1,34	1
W/L ratio	0,14	2
L/H ratio	5,4	1
z_0 [m]	0,005	4
windward 210°	yes	2
angle of attack 210°	13,8°	5
total		20

Table 4.1: Scoring process of a single cell using table 3.2

polygons) and *2)* multiple z_0 layers (geometry type: polygons). The functions then calculates the area and percentage of overlap between the cells of the VD and the z_0 layers. In Python, I assign the z_0 value of the highest percentage of overlap to the VC.

4.6 SCORING THE VORONOI DIAGRAM

After all the before mentioned implementations, most VCs now contain the calculated morphological parameters. Some cells did not receive a certain attribute due to limitation of the VD Algorithm 4.1. These cells are not considered in the scoring implementation.

The cells that have received all morphological parameter are scored using table 3.2. Table 4.1 is an actual example of the scoring of a VC.

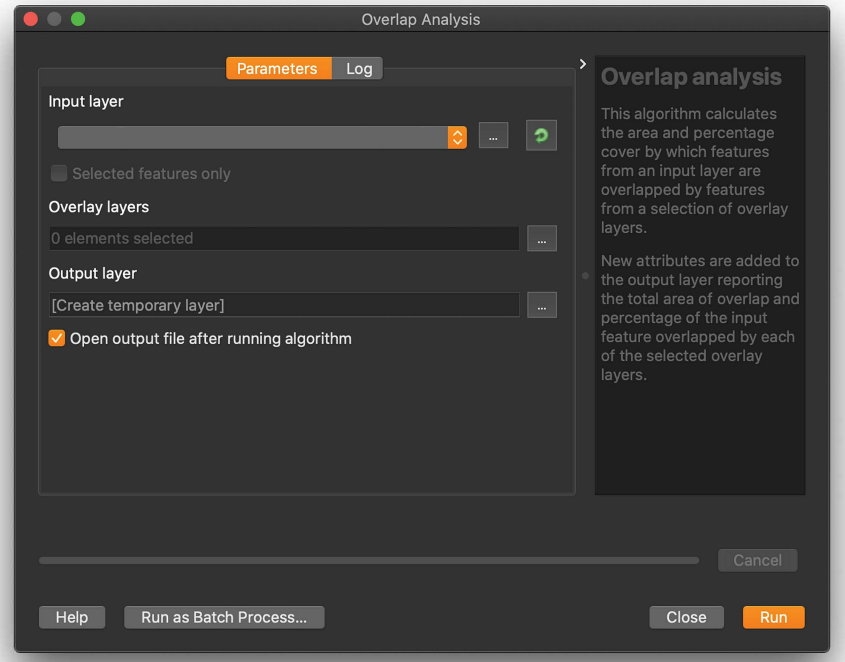

Figure 4.8: Function Overlap Analysis in QGIS3

5 RESULTS

In this chapter, I present the results of the implementations (§4). Here I also discuss how, based on the combination of different parameters, certain areas may have an increase potential in wind velocity.

5.1 MORPHOLOGY AROUND THE DELFSHAVEN STATION

The area around the station located on top op the building at Watergeusstraat, Delfshaven is presented here.

As visible in figure 5.1, the station is located on the outskirt of a neighborhood. The street widths are not as accurate due to the VD's cells being created using the neighborhood polygon. This only accounts for the cells created between the buildings and the neighborhood polygon. The cells between the buildings still provide accurate street widths. The widths are (ideally) towards the centre of the street. In the backyards, the VD is more irregular and therefore less precise in width calculation.

The result of the simple algorithm for the consecutive facade lengths (§3.6) is shown in figure 5.3. The results work for some facades better then for others. For example the facade on the line $x = 90350$ correctly displays the length of the facade in all cells, while for $y = 435600$ does not due to the saw-tooth like pattern in the facade.

In figure 5.4 the H/W ratio is colored according to the transition values for the different flows as described by Oke [1988]. Again, the area below the station is free from any buildings and so the H/W ratio is very low. North of the building the H/W ratio is still low. The buildings across from the meteorological station are taller, causing an asymmetric canyon.

The windward map (fig. 5.5) shows which facades are wind- or leeward, depending on the wind direction. In the figure, the wind direction is set to 240 compass degree. Figure 5.6 illustrates how the facades (and thus canyon) line up with the wind direction.

Figure 5.7 shows the area with it respective roughness length z_0. Most of the area around the station building is comprised of pavement. East of the building is a waterway, explaining the low z_0 values.

5.2 MORPHOLOGY AROUND THE CENTRUM STATION

It is important to note that the building across from the meteorological station (at junction 437475, 91825; fig. 5.8 to 5.12), was fully constructed around July of 2016. This has impact on a few things: 1) the meteorological data from the Centrum station is not representative of the current situation. 2) The Light Detection And Ranging (LiDAR) scan that was done to create the AHN3, was done before the construction of the new building. And as a result, the 3D BAG dataset that I am using, also does not contain the new building height information. In addition to this, the building is on the edge of the neighborhood polygon and is therefor not taken into account at the final scoring of the parameters.

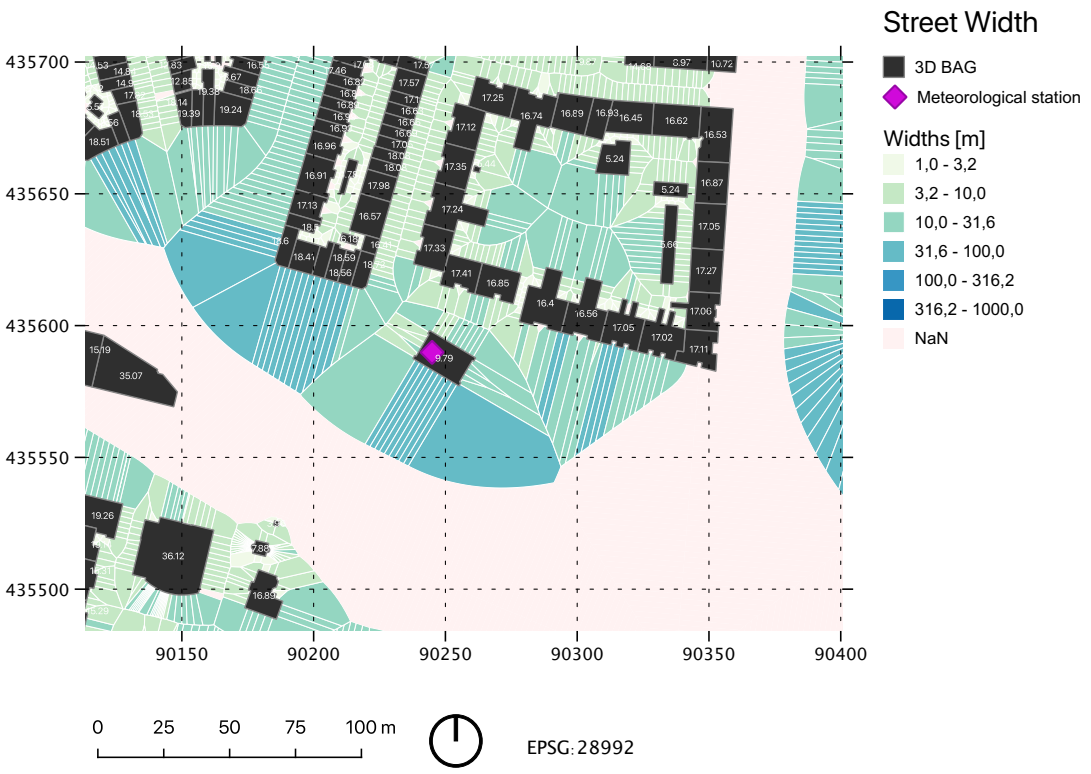

Figure 5.1: Street widths around the Delfshaven station

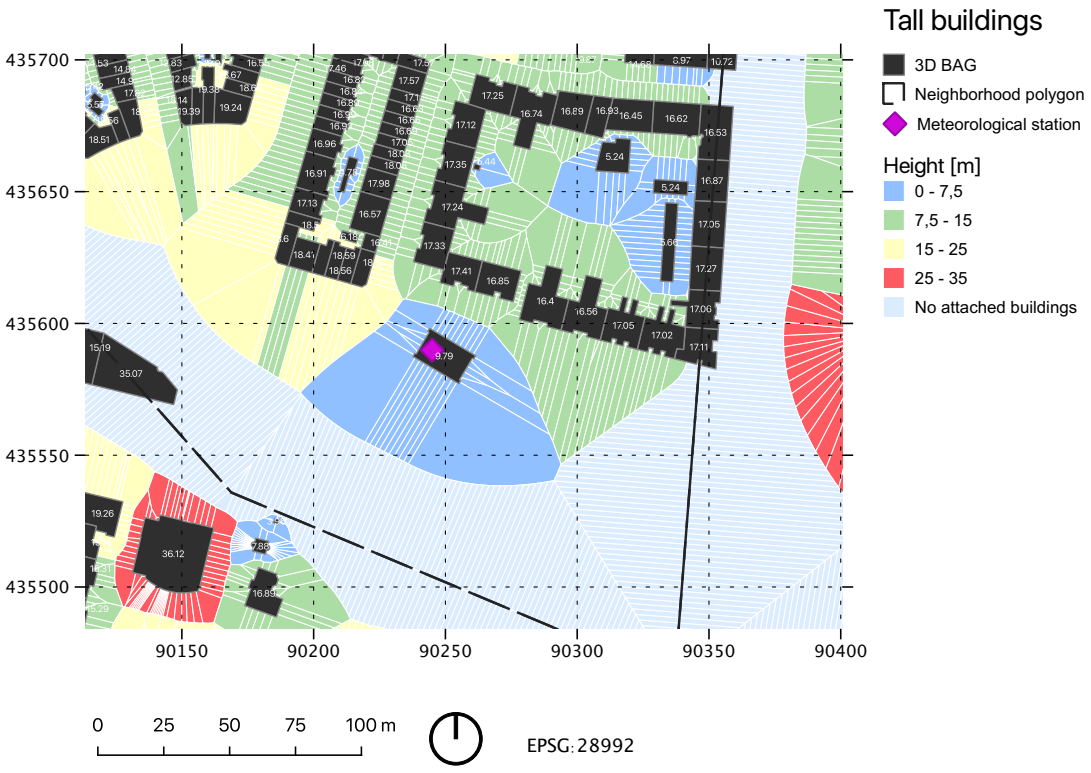

Figure 5.2: Tall buildings and height around the Delfshaven station

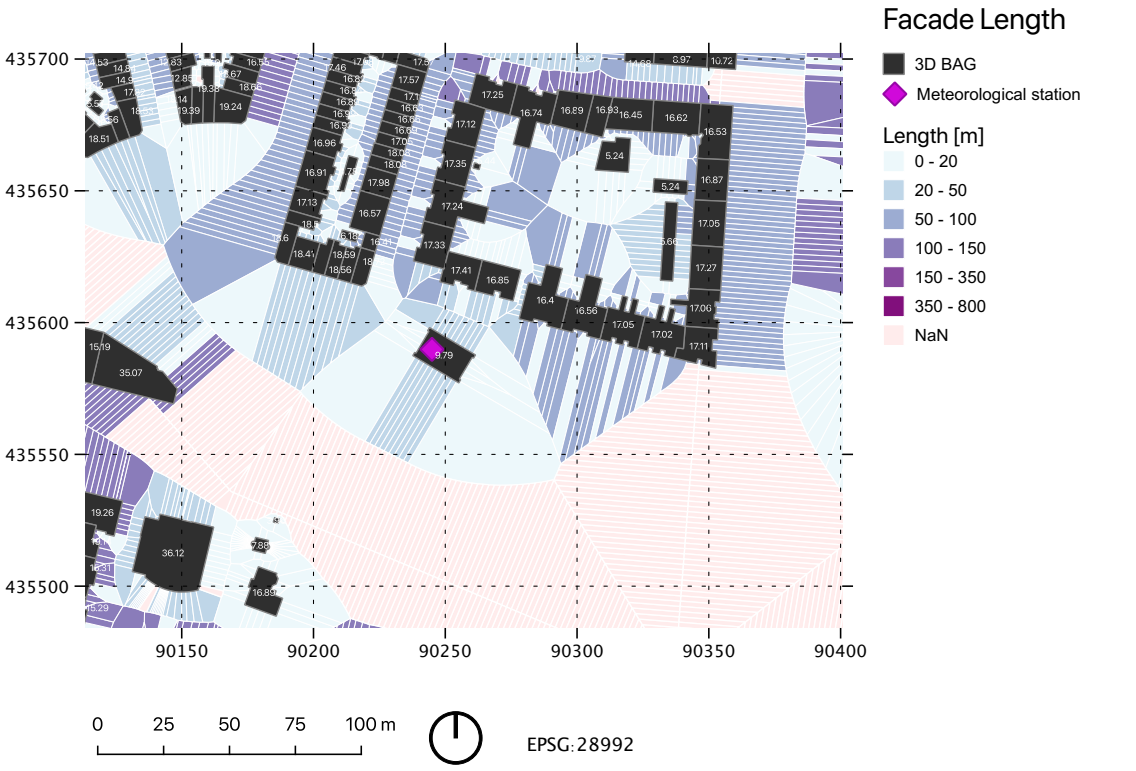

Figure 5.3: Facade lengths around the Delfshaven station

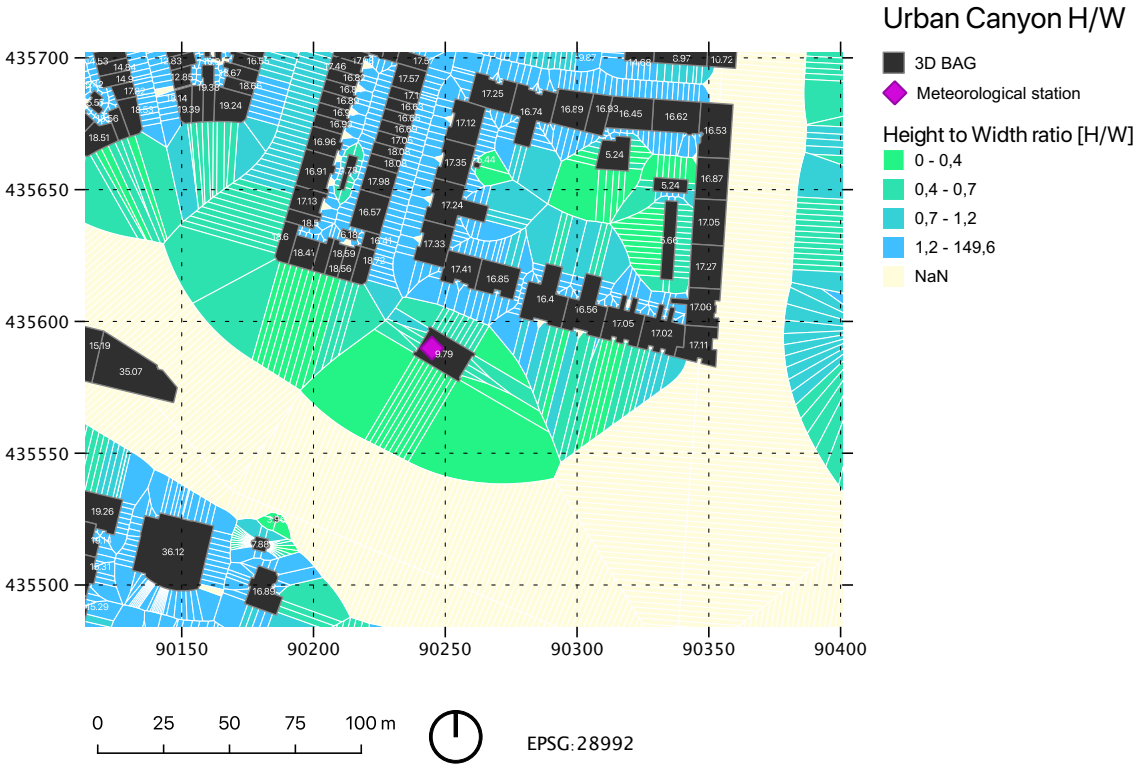

Figure 5.4: H/W ratio around the Delfshaven station

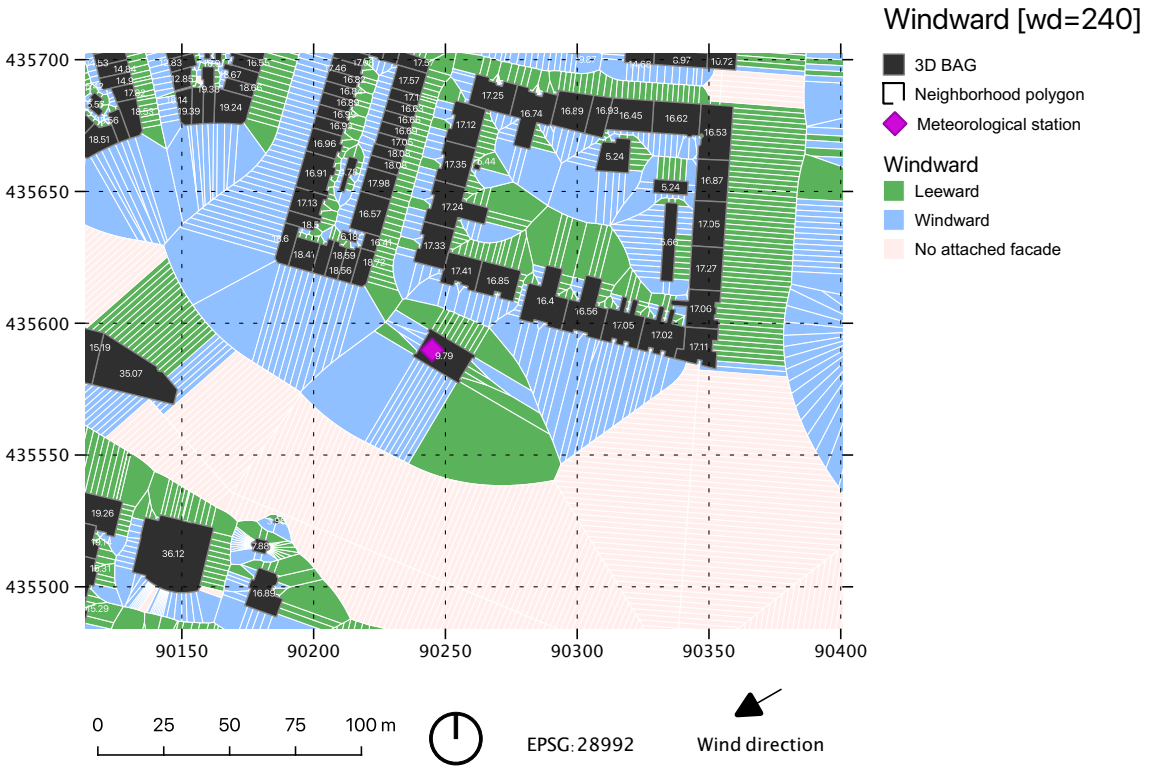

Figure 5.5: Wind- and leeward facades around the Delfshaven station for a wind direction of 240 compass degrees

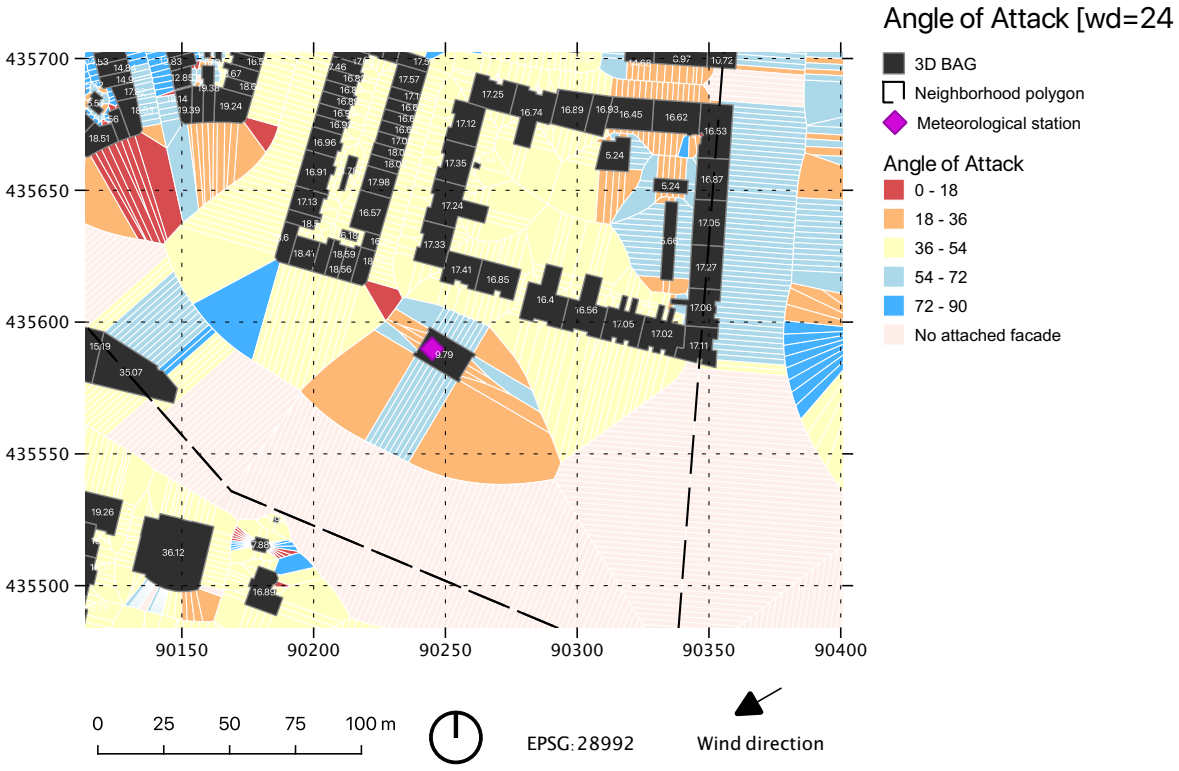

Figure 5.6: Angle of Attack around the Delfhaven station for wind direction of 240 compass degrees

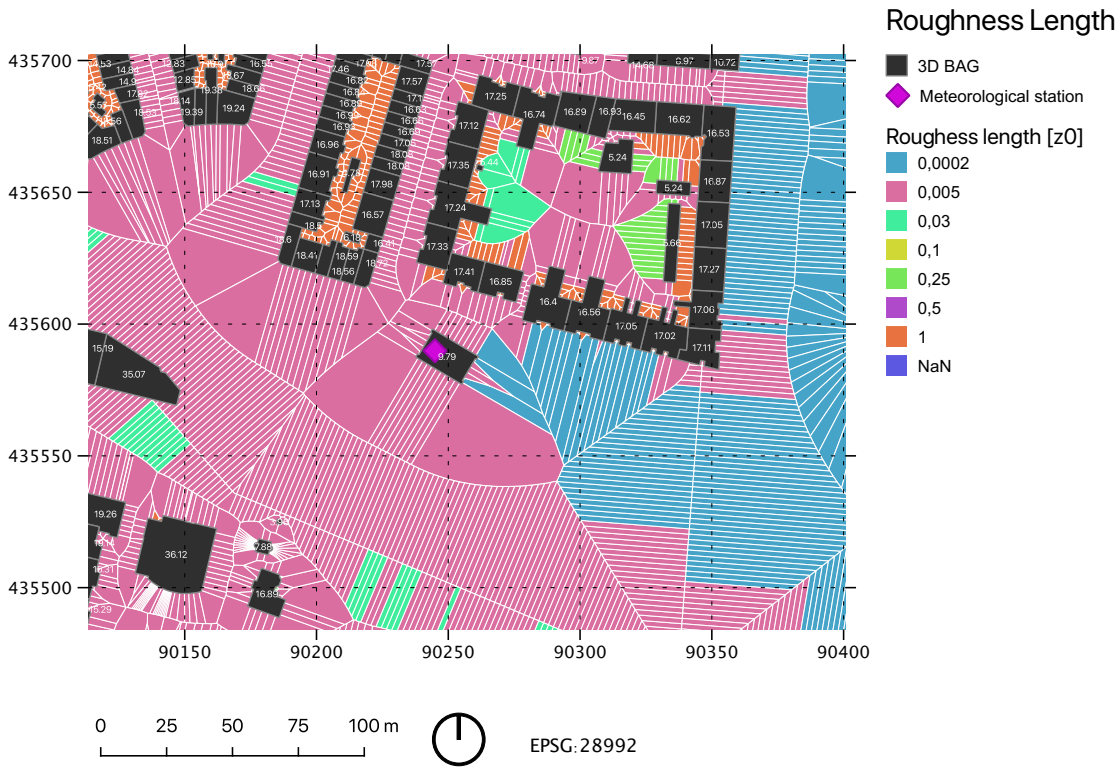

Figure 5.7: Roughness length around the weather station

Figure 5.8 shows the area around the Centrum station, with building height information in the intersecting VC. The meteorological station is situated very close to the tall building, illustrated by the red color.

The street widths are illustrated in figure 5.9. The neighborhood polygon, again, creates some issue here. Fortunately, the cell for meteorological station is still quite accurate. Measured in QGIS, the total distance from facade to facade is 57 meters (in this cade the VC width would be 28,5 meters), and the calculated VC width is 29 meters.

The canyon length is shown figure 5.10. Visible in this map are the setbacks in the facade causing 'breaks' in the VD. The lengths are nonetheless accurate, as the program takes these setbacks into account, and calculates the entire length of the building. The facade has a change in azimuth after approximately 70 meters, but the change is just under 20 degrees and is therefore grouped together.

Figure 5.11 shows the H/W values with corresponding transition values to the different flows as described in §2.1.2. Because of the neighborhood polygon, accuracy of this implementation is reduced for this section of the map.

Most of the area around the Centrum station consist of pavement with a z_0 value of 0.005, as visible in 5.12. The orange cells with a z_0 of 1 directly east of the meteorological station, are classified as private property. This is somehow due to the presence of a polygon labeled as private property (erf) inside the building.

Figure 5.13 illustrates the wind- and leeward facades for a wind direction of 240 compass degrees. For this wind direction, the facade next to the meteorological station is windward. And in figure 5.14 we can see that the wind direction lines up with the facade.

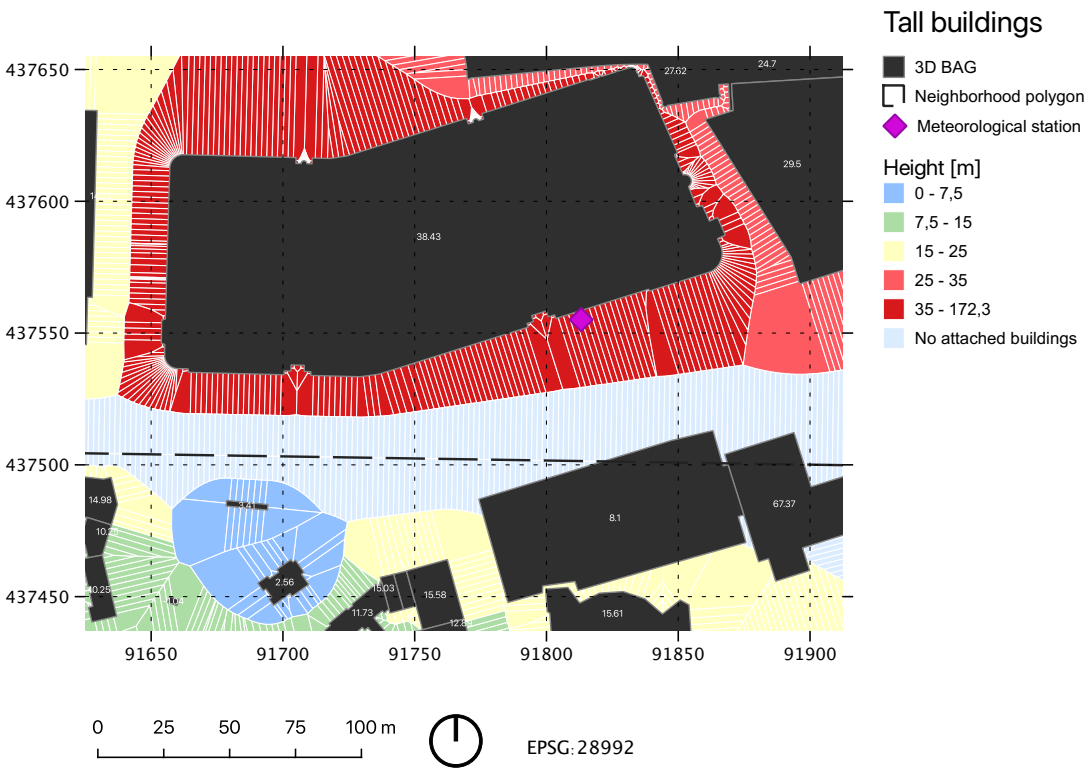

Figure 5.8: Tall buildings and height around the Centrum station

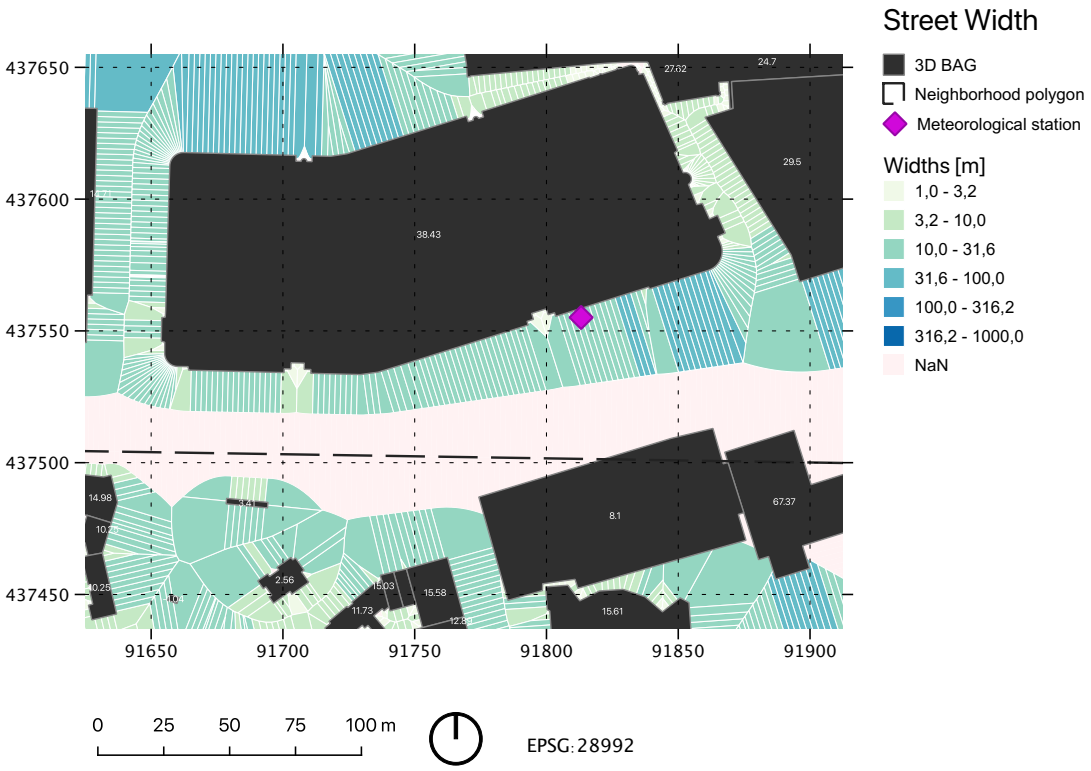

Figure 5.9: Street widths around the Centrum station

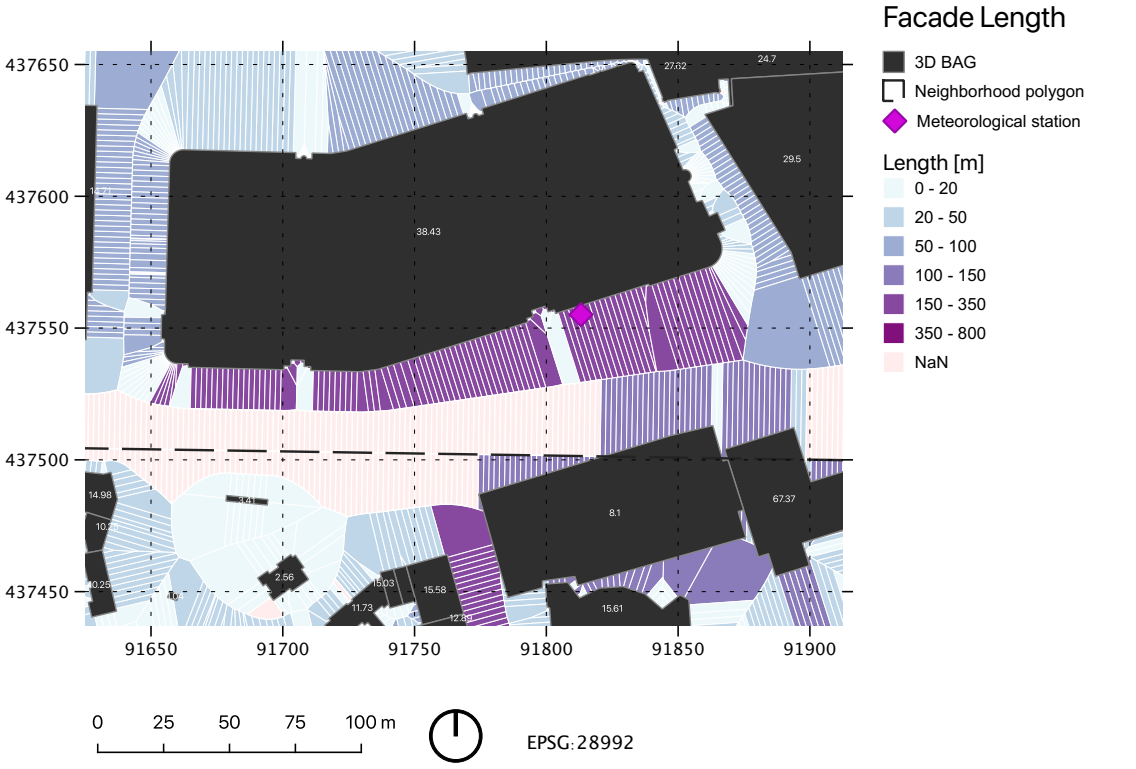

Figure 5.10: Facade lengths around the Centrum station

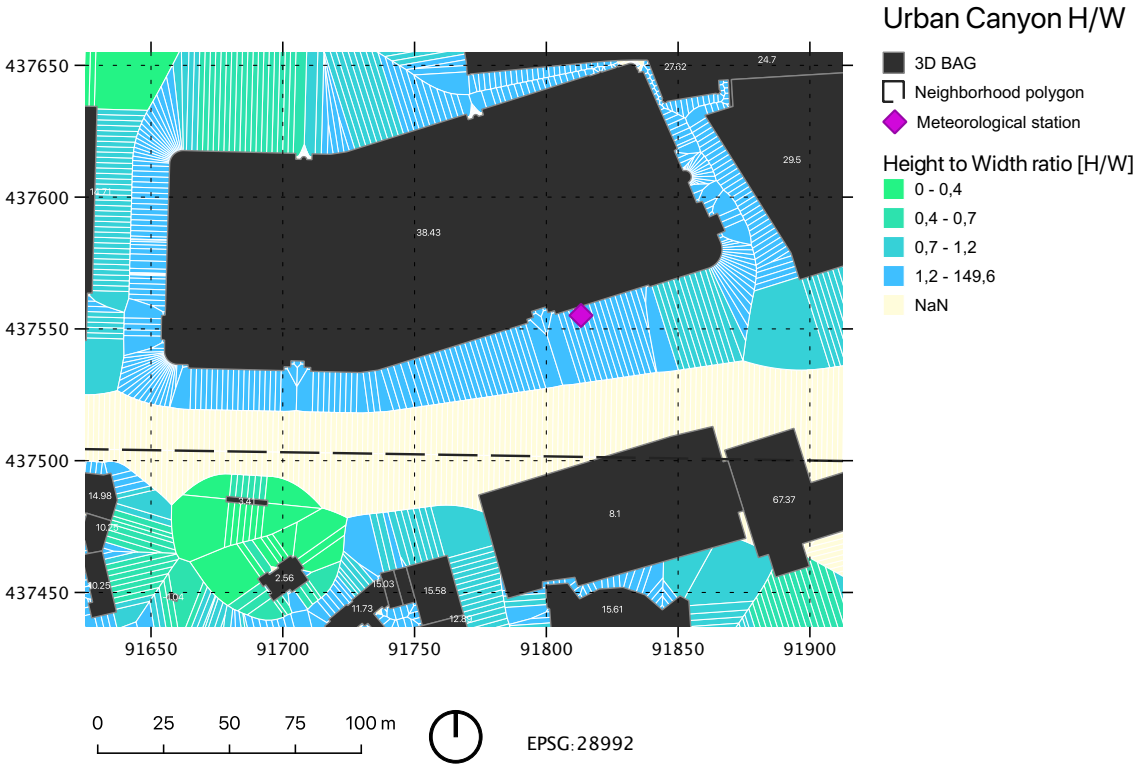

Figure 5.11: Height to Width ratio around the Centrum station

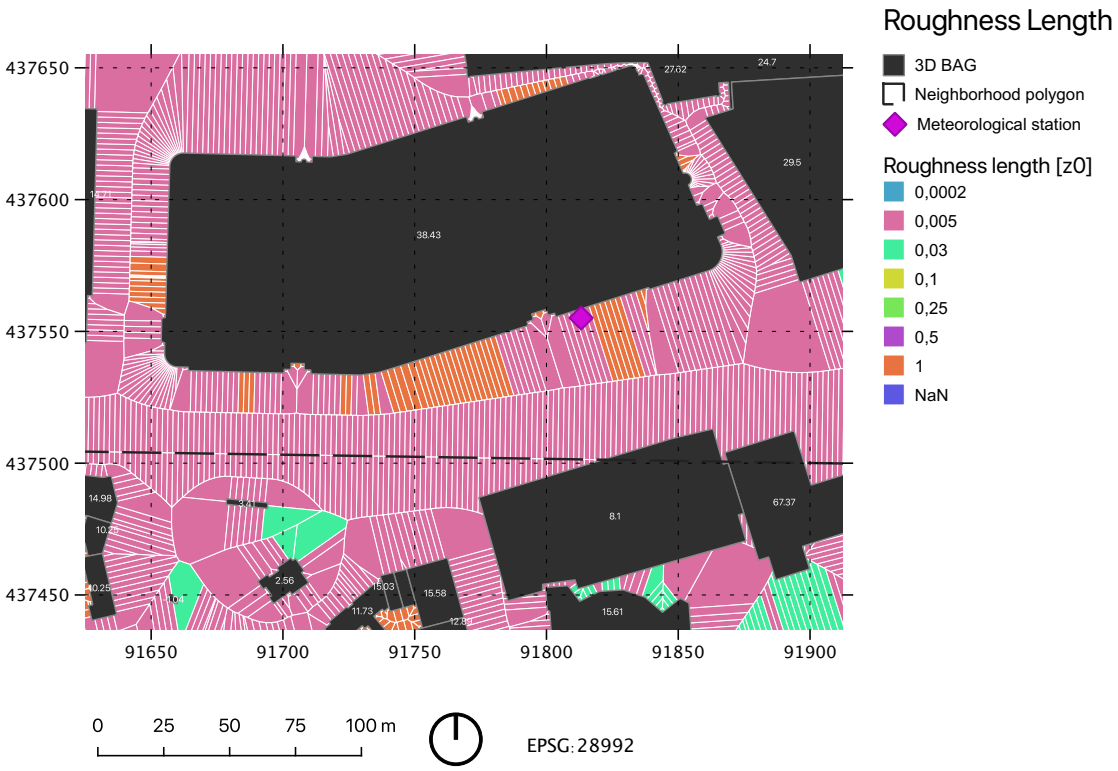

Figure 5.12: Roughness length values around the Centrum station

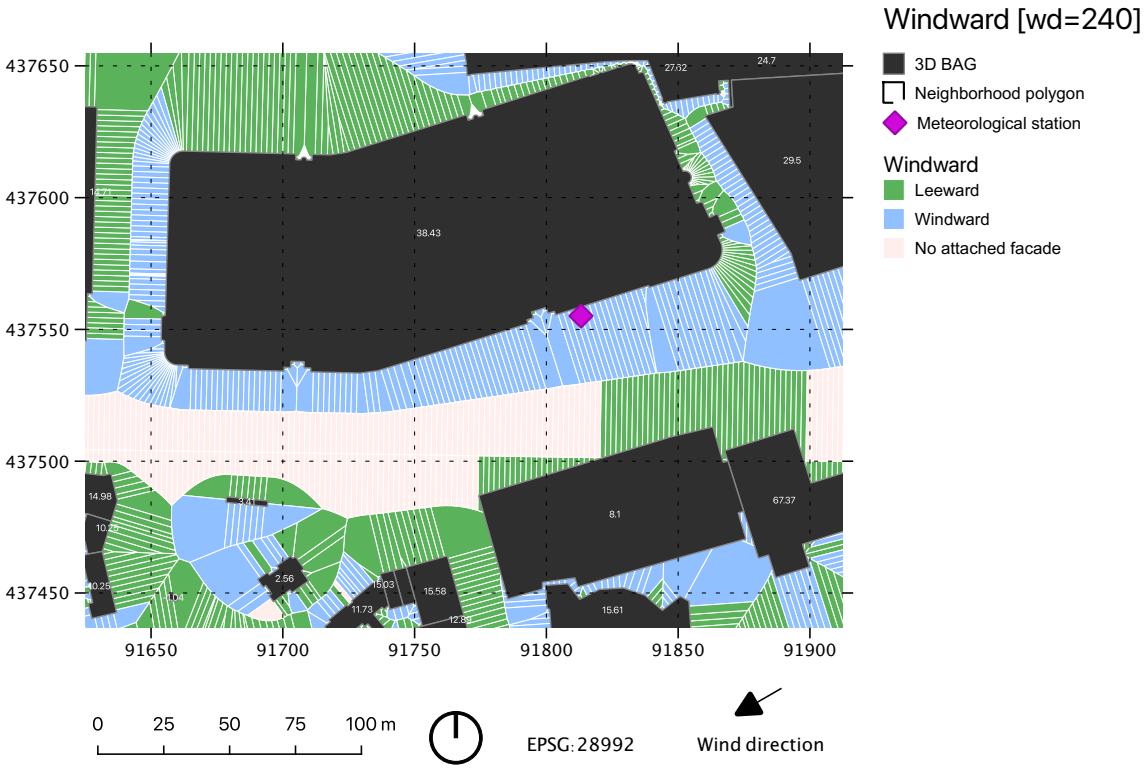

Figure 5.13: Wind- and leeward facades around the Centrum station for a wind direction of 240 compass degrees

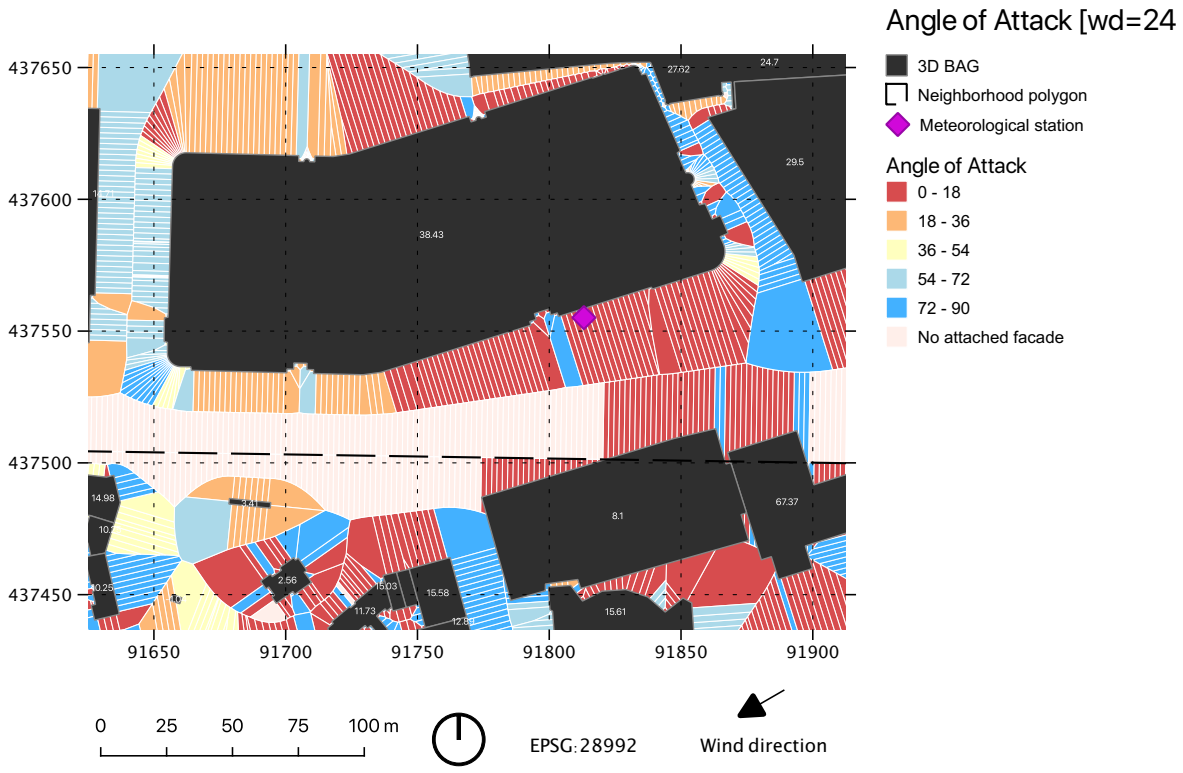

Figure 5.14: Angle of Attack around the Centrum station for wind direction of 240 compass degrees

5.3 SCORING THE VORONOI CELLS

Figures 5.15 and 5.16 show the calculated scores for each VC. Visible in the Delfshaven figure 5.15, are the presence of lower scores in this area, for this wind direction. While the cells around the Centrum station in figure 5.16, score higher due to the presence of taller buildings, longer canyon length and the azimuth of the facade lining up with the wind direction.

In the following tables (5.1 and 5.2) I have tried to validate the results using the urban station, the reference station and the scores for the 12 wind directions. The table is the output of the following query that can be formulated like this:

> Give me the measurements for both the reference and urban station, where the wind direction is 30 ±5 degrees and the reference station's wind speed is 1 ±0.1 m/s.

The columns in the tables can be described as follows:

- ***ref mean WS*** is the mean wind speed from the reference station's measurements, the resulted from the query.
- ***station mean WS*** is the mean wind speed of the measurements from the urban station, for that same moment in time of *ref mean WS*.
- ***# measurements*** are the amount of measurement that resulted from the query

In short, by comparing the score and the wind velocity at the urban station for different wind directions, we might be able to determine if the scores correlate with higher wind velocities. Figure 5.17 is a 3D bar graph visualisation of tables 5.1 and 5.2. In 5.17a. the higher scoring wind directions (illustrated by the lighter color

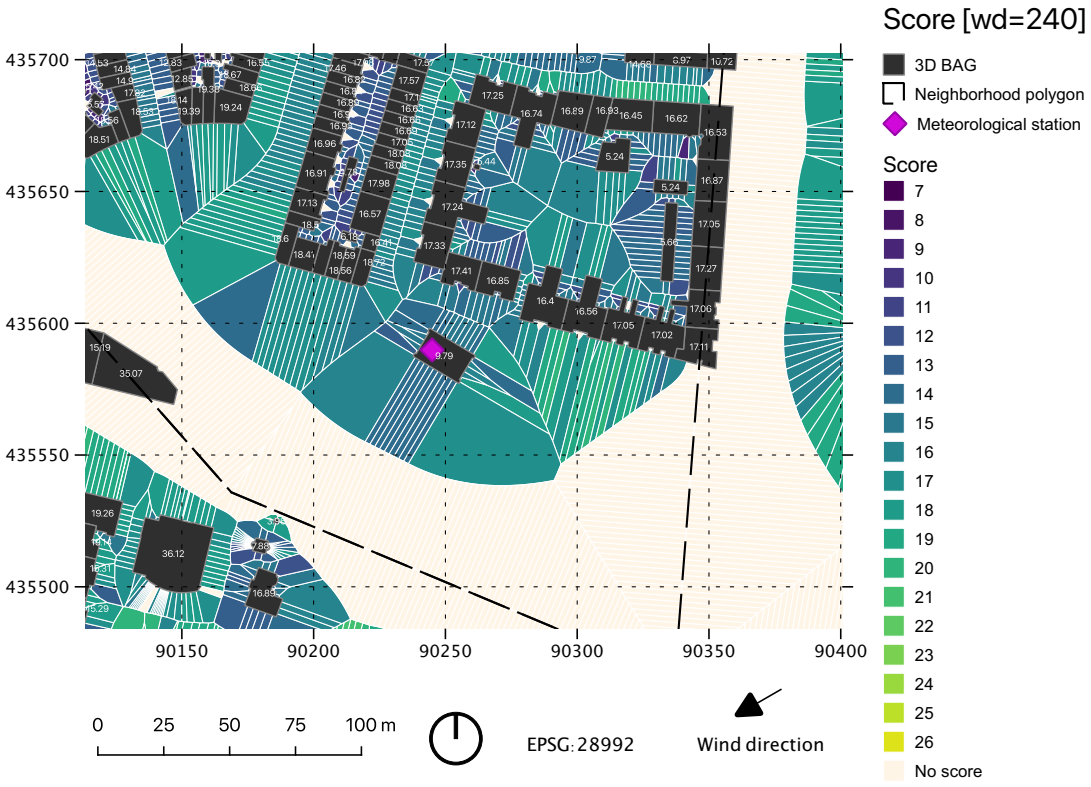

Figure 5.15: Morphology scores for wind potential around the Delfshaven station, for wind direction of 240 compass degrees.

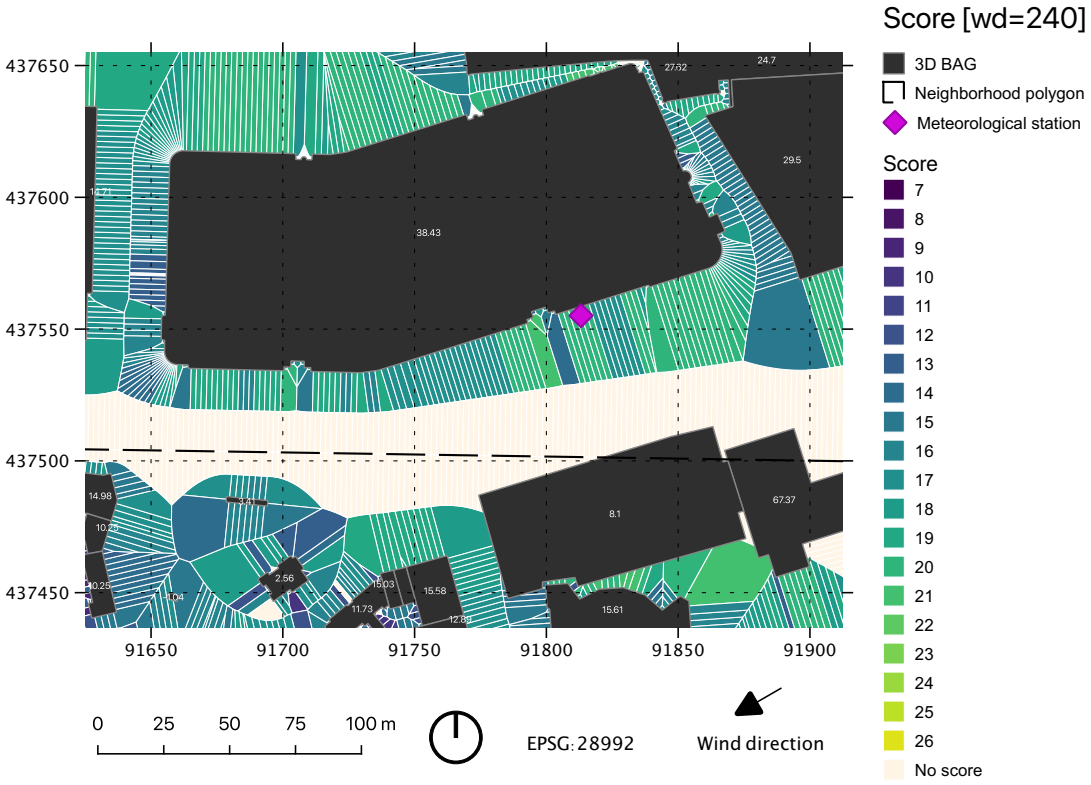

Figure 5.16: Morphology scores for wind potential around the Centrum station, for wind direction of 240 compass degrees.

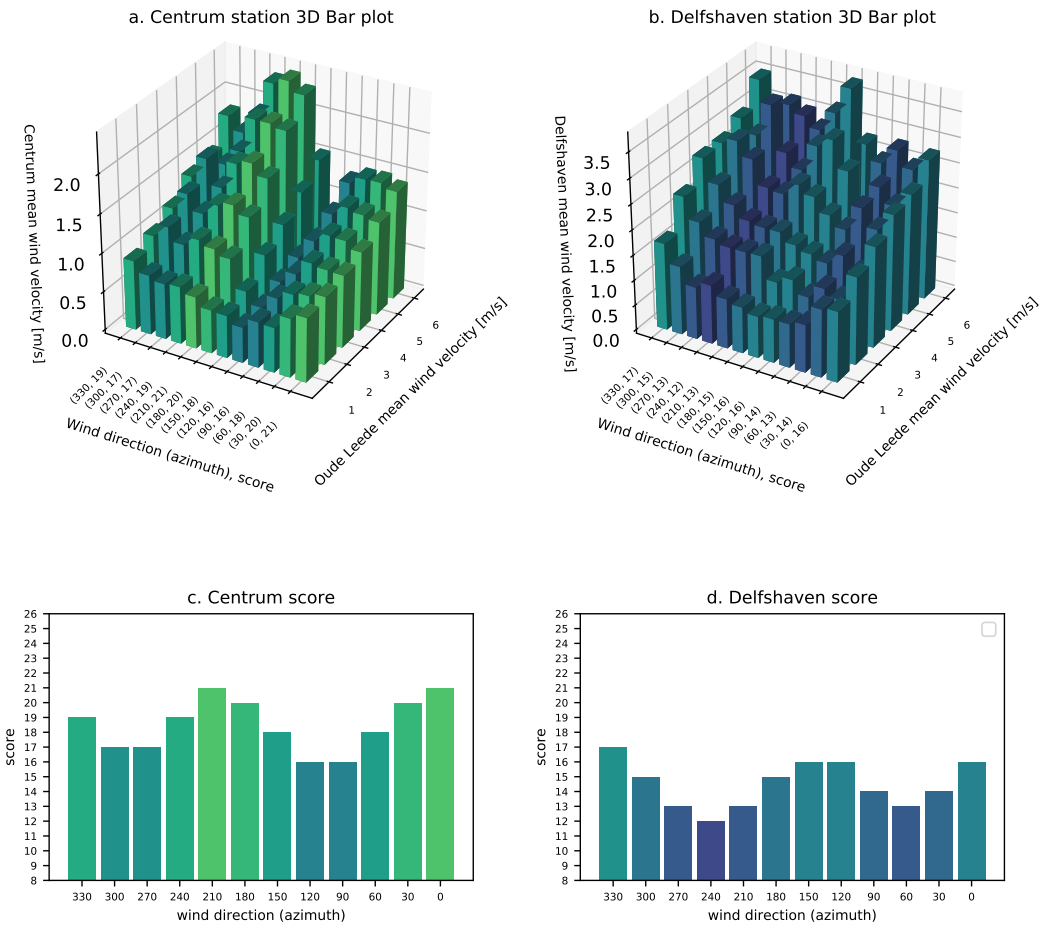

Figure 5.17: Top: a 3D bar graph with the x-axis showing the different wind direction and score, y-axis the mean wind velocity of the reference station Oude Leede and z-axis the mean wind velocity from the measurements of (a.) Centrum and (b.) Delfshaven. Bottom: a bar plot with the distribution of the scores for the twelve wind directions.

green) generally have a higher mean wind velocity compared to the lower scoring wind directions. Also, the lower scoring wind directions have lower mean wind velocities, especially so for wind direction 120.

The differences are not as clear in 5.17b. Although here, the highest scored wind direction (330 degrees) also consistently shows highest mean wind velocity for the reference wind velocity of 1, 2 and 3 and second highest for 4, 5 and 6. However, the lowest scored wind direction of 240 does not show lowest mean wind velocity.

However, due to the disparity between scale and resolution of the meteorological data and the VD area, this method of validation is not suitable. Trying to validate a model with an area of 9,2 km² with two stations located on two spots, is simply not possible. The outcome of this comparison does, hopefully, offer some incentive for future research.

I have now presented the scores only around the two meteorological stations. However, the scoring is done for the entire 9,2 km² area and can be used to determine other potential high velocity areas.

Table 5.1: Comparison of Delfshaven station and Oude Leede as a function of score and wind direction with ref WS selection range ±0.1

station	*reference station*	*query WD ref*	*score*	*station mean WS 1 ±0.1*	*ref mean WS 1 ±0.1*	*# measurements 1*	*station mean WS 2 ±0.1*	*ref mean WS 2 ±0.1*	*# measurements 2*	*station mean WS 3 ±0.1*	*ref mean WS 3 ±0.1*	*# measurements 3*	*station mean WS 4 ±0.1*	*ref mean WS 4 ±0.1*	*# measurements 4*	*station mean WS 5 ±0.1*	*ref mean WS 5 ±0.1*	*# measurements 5*	*station mean WS 6 ±0.1*	*ref mean WS 6 ±0.1*	*# measurements 6*
delfshaven	oude leede	0	16	1.40	1.00	60.0	1.74	2.00	78.0	2.01	3.00	68.0	2.32	4.01	58.0	2.41	5.00	20.0	2.79	5.98	12.0
delfshaven	oude leede	30	14	1.35	1.00	89.0	1.21	1.99	57.0	1.40	2.98	43.0	1.94	3.99	31.0	2.10	4.99	22.0	2.52	6.02	6.0
delfshaven	oude leede	60	13	0.95	0.99	77.0	1.33	2.00	103.0	1.66	3.01	50.0	2.28	4.00	28.0	2.39	5.02	16.0	2.82	6.01	6.0
delfshaven	oude leede	90	14	0.87	1.01	58.0	1.07	2.00	58.0	1.42	3.01	73.0	1.77	4.01	57.0	1.88	5.01	7.0	2.49	6.03	1.0
delfshaven	oude leede	120	16	0.87	1.00	66.0	1.32	2.00	54.0	1.51	3.00	70.0	1.97	4.00	53.0	2.54	4.99	19.0	2.78	5.97	6.0
delfshaven	oude leede	150	16	0.83	1.00	40.0	1.18	2.00	73.0	1.60	3.01	91.0	2.25	4.00	113.0	3.07	5.00	77.0	3.79	5.99	31.0
delfshaven	oude leede	180	15	0.92	1.00	170.0	1.61	2.01	90.0	1.77	2.99	121.0	2.40	4.01	150.0	2.87	5.00	148.0	3.24	6.01	91.0
delfshaven	oude leede	210	13	0.99	1.00	146.0	1.60	2.01	102.0	1.77	2.99	115.0	2.14	4.00	110.0	2.32	5.00	147.0	2.83	6.01	85.0
delfshaven	oude leede	240	12	1.17	1.01	58.0	1.60	2.01	105.0	1.82	2.99	93.0	2.18	3.99	70.0	2.58	4.99	55.0	3.03	6.01	19.0
delfshaven	oude leede	270	13	1.04	1.01	40.0	1.68	2.01	43.0	2.05	3.02	26.0	2.66	4.01	24.0	3.44	4.97	6.0	3.17	5.99	1.0
delfshaven	oude leede	300	15	1.36	1.00	33.0	1.93	2.00	82.0	2.37	3.02	60.0	2.94	3.99	21.0	2.77	5.00	5.0	NaN	NaN	0.0
delfshaven	oude leede	330	17	1.73	1.01	74.0	2.35	1.99	71.0	2.81	3.00	60.0	2.82	4.01	58.0	3.03	5.00	23.0	3.52	6.00	3.0

Table 5.2: Comparison of Centrum station and Oude Leede as a function of score and wind direction with ref WS selection range ±0.1

station	reference station	query WD ref	score	station mean WS 1 ±0.1	ref mean WS 1 ±0.1	# measurements 1	station mean WS 2 ±0.1	ref mean WS 2 ±0.1	# measurements 2	station mean WS 3 ±0.1	ref mean WS 3 ±0.1	# measurements 3	station mean WS 4 ±0.1	ref mean WS 4 ±0.1	# measurements 4	station mean WS 5 ±0.1	ref mean WS 5 ±0.1	# measurements 5	station mean WS 6 ±0.1	ref mean WS 6 ±0.1	# measurements 6
centrum	oude leede	0	21	0.83	1.00	144.0	0.88	2.00	145.0	0.94	3.01	122.0	1.03	4.00	93.0	1.21	5.01	47.0	1.40	5.97	3.0
centrum	oude leede	30	20	0.76	1.00	241.0	0.83	2.00	182.0	0.95	3.00	134.0	1.12	3.99	107.0	1.25	4.99	66.0	1.47	6.00	14.0
centrum	oude leede	60	18	0.58	1.00	203.0	0.79	2.00	259.0	0.98	3.00	197.0	1.13	4.00	102.0	1.29	4.99	66.0	1.46	6.00	14.0
centrum	oude leede	90	16	0.59	1.00	100.0	0.68	2.00	68.0	0.78	3.00	93.0	1.00	4.00	78.0	1.15	5.00	21.0	1.36	6.00	9.0
centrum	oude leede	120	16	0.46	1.00	174.0	0.50	1.99	135.0	0.62	3.00	100.0	0.73	4.00	85.0	0.76	5.01	52.0	0.85	5.99	38.0
centrum	oude leede	150	18	0.55	0.99	107.0	0.65	2.00	119.0	0.91	3.00	147.0	1.10	4.00	135.0	1.32	5.00	106.0	1.55	6.00	51.0
centrum	oude leede	180	20	0.56	1.00	289.0	1.01	1.99	218.0	1.34	3.00	273.0	1.64	4.00	279.0	2.06	5.00	226.0	2.33	6.00	202.0
centrum	oude leede	210	21	0.67	1.00	322.0	1.08	1.99	244.0	1.44	3.00	251.0	1.78	4.00	273.0	2.10	5.00	310.0	2.46	6.01	172.0
centrum	oude leede	240	19	0.74	1.00	138.0	1.14	2.00	318.0	1.38	3.00	345.0	1.72	4.00	228.0	2.10	5.00	192.0	2.38	6.00	145.0
centrum	oude leede	270	17	0.72	1.00	104.0	1.02	2.00	88.0	1.22	3.00	87.0	1.36	4.00	75.0	1.64	5.00	50.0	1.93	6.02	18.0
centrum	oude leede	300	17	0.77	1.01	76.0	1.19	2.01	105.0	1.42	3.00	99.0	1.68	3.99	51.0	1.42	4.96	15.0	1.65	6.01	7.0
centrum	oude leede	330	19	0.90	1.00	114.0	1.02	2.00	153.0	1.18	3.00	177.0	1.40	4.00	97.0	1.47	5.01	58.0	1.82	6.00	13.0

6 CONCLUSION AND FUTURE WORK

This thesis aims to answer the research questions presented in §1.1. I will answer these questions in the following section (§6.1). Afterwards, I will provide a discussion of the overall value of this thesis (§6.2). Finally, I give my recommendations for future work in §6.3.

6.1 RESEARCH OBJECTIVES

How do different morphological parameters relate to wind velocity? According to the research, the following parameters effect wind flows in the urban environment:

- **urban canyon parameters**, describing the height, width and length of the urban canyon. Different ratio's of these parameters lead to three different wind regimes inside the canyon, namely isolated roughness flow, wake interference flow and isolated skimming flow.
- **tall buildings**, where the flow of wind is being push down and generating increased pressure and velocity at pedestrian level.
- **orientation** of the canyon in relation to the wind direction, introducing a wind- and leeward side of the canyon and potentially channeling of wind flows.
- **terrain roughness length** causing an increase in turbulence and often a clear reduction in wind velocity, but open bodies of water or smooth pavement may limit the turbulence and drag factors.

How can we develop a methodology to compute multiple morphological parameters? After creating the VD base map, each parameter required a different approach to calculate:

- **heights** were provided in the 3D BAG dataset created by the 3D Geo-information team of TU Delft, that used the AHN3 dataset to extract building heights. To determine the threshold height of tall buildings, I looked at Dutch governments classification of tall buildings and the distribution of building height in the area of interest. From here, I classified buildings with a height exceeding a threshold of 23 meters as tall.
- **widths** were calculated using the following workflow:
  1. For each building, find surrounding VCs.
  2. Subtract the building geometry from the edges of the VC to obtain a representative line from the facade to the middle of the street.
  3. Assign the length of the line (describing the street width) to the VC's attributes.
- **lengths** were calculated using a backwards-looking facade algorithm that works as follows:
  1. Merge the footprint of the individual buildings into building blocks and simplify the resulting geometry to reduce amount of vertices using GIS operations.
  2. Calculate the azimuth for each individual line in the merged footprint.

3. Start the recursion: for every subsequent line, look at the previous four lines and compare the azimuth for the current. If they are similar, group them together.
4. Reiterate over all of the lines to calculate and assign the total facade lengths to the corresponding VC's attributes.

- **wind- or leeward facades** approach uses the merged footprint mentioned in step 1. and the azimuth in step 2. in the lengths methodology above. But instead of comparing the azimuth with the previous lines, it compares the azimuth with the wind direction and makes use of the footprints geometrical organisation to determine wind- and leeward sides of the building block. For the purpose of this thesis, the wind- and leeward facades are calculated for 12 distinct wind directions, covering 0 to 360 degrees (0, 30, 60, etc.).

- **angle of attack** is calculated by determining the angle between the azimuth of the building block facade and the 12 wind directions from 0 to 360 degrees. These values are then assigned to the corresponding VC.

- **roughness length** is determined as follows:
  1. The BGT dataset is subdivided into separate layers, according to the Davenport classification for roughness length (table 3.1).
  2. Using QGIS3 function Overlay Analysis, the area [m²] and percentage of overlap between the BGT sub-layers and every VC is calculated.
  3. Then, for every VC the highest overlap percentage with the BGT sub-layer is given the corresponding roughness value z_0 from table 3.1.

Is this method suitable for identifying potentially increased wind velocity situations? I have tried to find a way to combine the calculated morphological parameters into an indicator for wind velocity potential. By using thresholds, I score every parameter either 5 to 1 or 3 to 1. Because the potential changes with regards to wind direction, every VC receives 12 different scores where the difference is mainly due to the *wind- and leeward* and *angle of attack* parameters.

After determining the scores for the 12 separate wind directions, I use the available meteorological stations to look at local wind velocities. Per wind direction, I expect to see if the highest score matches roughly the highest wind velocity and/or if the lowest score matches to lowest wind velocity at the urban meteorological stations.

Can we use measurements from meteorological stations to validate the methodology? Even though the measurements of the two urban stations (Centrum and Delfshaven) do not have overlapping time frames, the data can still be used to provide an indication. The comparison is done between a reference station outside the area and the urban stations within the area of interest. Here, the mean wind velocity at the urban station is calculated for 12 wind directions (0 to 360 degrees) and 6 velocities (1 to 6 m/s) at the reference station.

The comparison indicates a higher mean wind velocity for the higher scoring wind directions for both station. The Centrum station also shows lower mean wind velocity for the lowest scoring wind direction. However, a better approach is necessary in order to determine the validity of the scoring method.

Can we use urban morphology to automatically calculate potential increase in wind velocity? The answer to the main research question lies in a combination of the sub-questions answered above. Firstly, I have demonstrated that by using open data and tools, several urban morphological parameters related to wind velocity can be computed. The calculation of the parameters is done automatically, apart from the data preparation and the steps between methodologies which are done manually.

Secondly, I introduced a simple scoring method to link urban morphology to potential increase wind velocity. The method uses the calculated parameters from different implementations, and assigns a score based on different parameter thresholds. The result is a VD of the urban environment, comprised of scored VCs, where a higher score indicates a higher probability of potential increased wind velocity.

Thirdly, by comparing two meteorological stations with the scored cells they are located in, we notice that for one station (Centrum) the higher wind velocities match the higher scores and vice versa. For the other station (Delfshaven), this relationship is less apparent. However, the highest score does match with the highest mean wind velocity. The outcome of this comparison is an incentive for future research.

To conclude, in this thesis I set out to explore methodologies to compute multiple urban morphological analysis related to potential increase in wind velocity. The result of this thesis shows that the calculation of the parameters is possible. However, the translation from urban morphology to potential increase in wind velocity requires more exploration.

6.2 DISCUSSION

A significant portion of this thesis is related to the calculation of the morphological parameters. One of the mayor goals of this thesis is to relate these parameters to potential increase in wind velocities. To relate these parameters to wind velocity conditions, a 'simple' score system is used. This method of scoring the parameters could be done in a multitude of different ways and is thus not an accurate representation of the complex, real-world conditions. However, it should be noted that this is indeed not what that intention of this thesis really is, as mentioned in the introduction. Because the intention would be using the combination of parameters as an indicator for potential wind velocity increased situations. And hopefully using certain areas with high scores as potential areas of interest for future wind measurements or simulations.

For validating the scoring method, meteorological stations are used and compared. However, the time frames of the two urban stations do not line-up, and therefore a real-time comparison of the measurements is not possible. This thesis is dependent on and limited by open data and I have to work with what is available.

I created a script and workflow that requires minimal user input. However, I noticed that I was a lot more dependent on QGIS operations than I originally set out to be. Causing some parts of the methodologies to be done by hand; especially the roughness length methodology. Nonetheless, the calculation of the parameters was done automatically (or without user input) and only preparing and harmonising the data into the VD was done manually using QGIS operations.

Further limitations of the methodology are as follows:

- The width calculation only makes use of the VC's edges that intersect with the buildings, as this is the closest distance to another facade. However, in more open areas, such as squares, the VC usually does not intersect with another edge that is representable for another facade. As a consequence, the street width is misinterpreted.

- Because a VC usually has two edges intersecting a building, I've taken the mean of the two edge lengths to represent street width for that cell. However, when encountering building corners, where a narrow street is perpendicular to a wide street, the street width does not represent either street e.g. $(2 + 14)/2 = 8$.

- The VD handles neatly organised geometry for streets well, but chaotic building environment causes chaotic VCs. This mainly impacts the canyon width calculation, as explained in the previous point.
- Using facade length to represent the length of the urban canyon is experimental. I have not found any documentation about this and arguments can be made in favor and against.
- The facade length code is simple and robust, but complexity could be added to increase the quality of the result.
- Use of the neighborhood polygon speeds up computation time and memory space, but as a consequence some VCs are not considered for the scoring system. This results in a map with some areas not receiving a score indicating potential increase of wind velocity.
- The implementation looks at the geometry of the built and non-built space, and so does not take trees or other objects into account, although they have shown to impact wind velocity in the urban canopy layer. In the Netherlands, most trees are 'registered' and so trees can be incorporated
- The windward and AOA implementation examines only the line itself, and does not consider objects that might be up-wind and blocking the facade.

6.3 FUTURE WORK

First, improvements could be made on the different implementations. Starting with the creation of the VD, where using neighborhood polygons for creating subsets of the area posed issues for morphological calculations. It could be investigated if using subsets for the area is necessary and instead create one VD for the entire area. This way, the problem where the edges are not classified in the current method, is solved. Though, trying to create one VD for the area might depend on the available RAM storage of the device running the algorithm.

Second, improvements could be made to the canyon length algorithm. Possibly by adding more complexity, such as measuring the length of a setback, a better distinction could be made as to what constitutes as a continuous facade.

The windward and AOA implementation could be improved by also considering buildings up-wind. In the code published on GitHub is an algorithm that computes the wind shadow, determined by the building height, leeward side and wind direction. By overlapping the shadows with the windward facades or the VCs, distinction between free and obstructed facades could be made.

The implementation is now done only for the research area in Rotterdam, but should be able to run for other cities in the Netherlands as well. If CFD simulations done for other urban areas in Dutch cities, the method proposed in this thesis might offer additional insight. Not just the score system, but the various morphological parameters can be used to classify the urban canyons for urban analysis.

This methodology can be used in general urban morphological analysis and for a variety of (specialised) use cases. This thesis presents only one, potential wind velocity, but the morphological parameters (especially canyon height, width and length) can be used for noise calculation, pollution levels, energy balance and for numerous other fields.

BIBLIOGRAPHY

Adolphe, L. (2001). A simplified model of urban morphology: Application to an analysis of the environmental performance of cities. *Environment and Planning B: Planning and Design*, 28(2):183–200.

Arnold, S., Apsimon, H., Barlow, J., Belcher, S. E., Bell, M., Boddy, J., Britter, R., Cheng, H., Clark, R., Colvile, R., Dimitroulopoulou, C., Dobre, A., Greally, B., Kaur, S., Knights, A., Lawton, T., Makepeace, A., Martin, D., Neophytou, M., and Walsh, P. (2004). Introduction to the dapple air pollution project. *The Science of the total environment*, 332:139–53.

Badach, J., Voordeckers, D., Nyka, L., and Van Acker, M. (2020). A framework for air quality management zones - useful gis-based tool for urban planning: Case studies in antwerp and gdańsk. *Building and Environment*, 174:106743.

Beranek, W. and Koten, H. V. (1979). *Beperken van windhinder om gebouwen, deel 1, Stichting Bouwresearch no. 65*. Kluwer Technische Boeken BV, Deventer.

Berghauser Pont, M. Y. and Haupt, P. A. (2009). Space, density and urban form.

Blocken, B. and Carmeliet, J. (2004). Pedestrian wind environment around buildings: Literature review and practical examples. *Journal of Thermal Environment and Building Science*, 28(2):107–159.

Carpentieri, M. and Robins, A. G. (2015). Influence of urban morphology on air flow over building arrays. *Journal of Wind Engineering and Industrial Aerodynamics*, 145:61–74.

Ceccarelli, G., de Jongh, W., Lánský, I., Li, J., Mastorakis, K., Teeuwisse, S., Peters, R., Sanchez, C. G., and Stoter, J. (2019). Bepalen luchtverontreiniging door verkeer met behulp van 3d-geo-informatie. *Geo-Info*, 16(4):34–39.

Chen, L., Hang, J., Sandberg, M., Claesson, L., Sabatino, S. D., and Wigo, H. (2017). The impacts of building height variations and building packing densities on flow adjustment and city breathability in idealized urban models. *Building and Environment*, 118:344–361.

Claus, J., Coceal, O., Thomas, T. G., Branford, S., Belcher, S., and Castro, I. P. (2011). Wind-direction effects on urban-type flows. *Boundary-Layer Meteorol*, (142):265–287.

Fleischmann, M., Feliciotti, A., Romice, O., and Porta, S. (2020). Morphological tessellation as a way of partitioning space: Improving consistency in urban morphology at the plot scale. *Computers, Environment and Urban Systems*, 80:101441.

Janssen, W., Blocken, B., and van Hooff, T. (2013). Pedestrian wind comfort around buildings: Comparison of wind comfort criteria based on whole-flow field data for a compex case study. *Building and Environment*, 59:547–562.

Jhaldiyal, A., Gupta, K., Gupta, P. K., Thakur, P., and Kumar, P. (2018). Urban morphology extractor: A spatial tool for characterizing urban morphology. *Urban Climate*, 24:237–246.

Jiang, D., Jiang, W., Lui, H., and Sun, J. (2008). Systematic influence of different building spacing, height and layout on mean wind and turbulent characteristics within and over urban building arrays. *Wind and Structures*, 11(4):275–289.

Kubota, T., Miura, M., Tominaga, Y., and Mochida, A. (2008). Wind tunnel tests on the relationship between building density and pedestrian-level wind velocity: Development of guidelines for realizing acceptable wind environment in residential neighborhoods. *Building and Environment*, 43(10):1699–1708.

Memon, R. A., Leung, D. Y., and Liu, C.-H. (2010). Effects of building aspect ratio and wind speed on air temperatures in urban-like street canyons. *Building and Environment*, 45(1):176–188.

Mou, B., He, B.-J., Zhao, D.-X., and wing Chau, K. (2017). Numerical simulation of the effects of building dimensional variation on wind pressure distribution. *Engineering Applications of Computational Fluid Mechanics*, 11(1).

Oke, T. R. (1988). Street design and urban canopy layer climate. *Energy and Buildings*, 11:103–113.

Oke, T. R., Mills, G., Christen, A., and Voogt, J. A. (2017). *Urban climates*. Cambridge University Press.

Park, S.-J., Kim, J.-J., Choi, W., Kim, E.-R., Song, C.-K., and Pardyjak, E. R. (2019). Flow characteristics around step-up street canyons with various building aspect ratios. *Boundary-Layer Meteorology*, 174:411–431.

Razak, A. A., Hagishima, A., Ikegaya, N., and Tanimoto, J. (2013). Analysis of airflow over building arrays for assessment of urban wind environment. *Building and Environment*, 59:56–65.

Rijksoverheid (2021).

Roberts, S. A., Hall, G. B., and Boots, B. (2005). Street centreline generation with an approximated area voronoi diagram. In *Developments in Spatial Data Handling*, pages 435–446, Berlin, Heidelberg. Springer Berlin Heidelberg.

Samsonov, T. E., Konstantinov, P. I., and Varentsov, M. I. (2015). Object-oriented approach to urban canyon analysis and its applications in meteorological modeling. *Urban Climate*, 13:122–139.

Soulhac, L., Garbero, V., Salizzoni, P., Mejean, P., and Perkins, R. (2009). Flow and dispersion in street intersections. *Atmospheric Environment*, 43(18):2981–2996.

Soulhac, L., Perkins, R., and Salizzoni, P. (2008). Flow in a street canyon for any external wind direction. *Boundary-Layer Meteorology*, 126:365–388.

Tsang, C., Kwok, K., and Hitchcock, P. (2012). Wind tunnel study of pedestrian level wind environment around tall buildings: Effects of building dimensions, separation and podium. *Building and Environment*, 49:167–181.

Wieringa, J. (1986). Roughness-dependent geographical interpolation of surface wind speed averages. *Quarterly Journal of the Royal Meteorological Society*, 112(473):867–889.

Wieringa, J. (1992). Updating the davenport roughness classification. *Journal of Wind Engineering and Industrial Aerodynamics*, 41(1):357–368.

Xie, X., Liu, C.-H., and Leung, D. Y. (2007). Impact of building facades and ground heating on wind flow and pollutant transport in street canyons. *Atmospheric Environment*, 41(39):9030–9049.

Zajic, D., Fernando, H. J. S., Calhoun, R., Princevac, M., Brown, M. J., and Pardyjak, E. R. (2011). Flow and turbulence in an urban canyon. *Journal of Applied Meteorology and Climatology*, 50(1):203 – 223.

Zhang, Y., Ou, C., Chen, L., Wu, L., Liu, J., Wang, X., Lin, H., Gao, P., and Hang, J. (2020). Numerical studies of passive and reactive pollutant dispersion in high-density urban models with various building densities and height variations. *Building and Environment*.

COLOPHON

This document was typeset using LaTeX. The document layout was generated using the arsclassica package by Lorenzo Pantieri, which is an adaption of the original classicthesis package from André Miede.